Supporting Information File

Environment-friendly, Cocatalyst-free Chemical Fixation of CO_2 at Mild Conditions Using Dual-walled Nitrogen-rich 3D Porous Metal-Organic Frameworks (MOFs)

Bharat Ugale, Sandeep Kumar, T. J. Dhilip Kumar and C. M. Nagaraja*

Department of Chemistry, Indian Institute of Technology Ropar, Rupnagar 140001, Punjab, India.Tel: 91- 1881-242229.Email: cmnraja@iitrpr.ac.in

Contents:

1. **X-ray Crystallography**
2. **Table S1**. Crystal data and structure refinement parameters for **1** and **2**.
3. **Table S2** Selected bond lengths (Å) and angles (°) for MOF**1.**
4. **Table S3**. Selected bond lengths (Å) and angles (°) for MOF**2**.
5. **Figure S1.** PXRD patterns of MOF**1** (a) pattern calculated from single crystal X-ray data, (b) as-synthesized sample, (c) activated sample by heating at 150 ºC under vacuum for 20 hours.
6. **Figure S2.** FT-IR spectrum for MOF **1** and **2** and their activated samples.
7. **Figure S3.** PXRD patterns of MOF**2** (a) pattern calculated from single crystal X- ray data, (b) as-synthesized sample, (c) activated sample by heating at 150 ºC under vacuum for 20 hours.
8. **Figure S4.** Space-filled view of the cage-A (a), for cage-B (b), and for dual-walled cage formed by encapsulation of cage-B into cage-A (c). (d) TOPOS representation of 3D framework in **1** and **2** with 2-fold interpenetration (two different colors are used to

represent two different nets). (e) pi-pi interactions present between two nets which are 3.456 Å far from each other.

9. **Figure S5.** Powder XRD patterns of MOF**1** isolated after treating with different solvents.
10. **Figure S6.** Powder XRD patterns of MOF**1** isolated after treating with different pH conditions.
11. **Figure S7.** N_2 adsorption-desorption isotherms at 77K for MOF**1** and MOF**2.** Closed circles represents adsorption and open circles for desorption.
12. **Figure S8.** CO_2 adsorption-desorption isotherms carried out at 273 and 298K for MOF**1**.
13. **Figure S9.** Carbon dioxide adsorption isotherm for MOF**1** at 273 K. The solid line shows the best fit to the data using Langmuir- Freundlich Equation.
14. **Figure S10.** Carbon dioxide adsorption isotherm for MOF**1** at 298 K. The solid line shows the best fit to the data using Langmuir- Freundlich Equation.
15. **Figure S11.** Enthalpy of carbon dioxide adsorption for MOF**1** using Clausius-Clapeyron Equation calculations.
16. **Figure S12.** Gas selectivity for MOF**1** calculated following the Henry's law from the CO_2, N_2, Ar and H_2 isotherms at 273K.
17. **Figure S13.** Optimized structure of $TATAB^{3-}$ ligand coordinated to a paddlewheel $Co(OOC)_2(H_2O)_2$ SBU. Atom colors: Co-green; C-dark grey; O-Red; H-white and N-blue.
18. **Table S4.** Optimization of reaction parameters for CO_2 cycloaddition with epichlorohydrin.
19. **Figure S14.** ^1H NMR ($CDCl_3$, 400 MHz) spectra for the cycloaddition reaction of epichlorohydrin with CO_2 using MOF**1** as catalyst (Table S4, entry no. 5).

20. **Figure S15.** ^{1}H NMR ($CDCl_3$, 400 MHz) spectra for the cycloaddition reaction of epichlorohydrin with CO_2 using MOF**1** as catalyst (Table 1, entry no. 2) & (Table 2, entry no. 1).
21. **Figure S16.** ^{1}H NMR ($CDCl_3$, 400 MHz) spectra for the cycloaddition reaction of epichlorohydrin with CO_2 using MOF**1** as catalyst (Table S4, entry no. 7) & (Table 1, entry no. 4).
22. **Figure S17.** ^{1}H NMR ($CDCl_3$, 400 MHz) spectra for the cycloaddition reaction of epichlorohydrin with CO_2 using MOF**1** as catalyst (Table S4, entry no. 8).
23. **Figure S18.** ^{1}H NMR ($CDCl_3$, 400 MHz) spectra for the cycloaddition reaction of epichlorohydrin using CO_2 and N_2 gases with pressure ratio of 2/6 (total of 8 bar) and MOF**1** as a catalyst (Table 1, entry no. 5).
24. **Figure S19.** ^{1}H NMR ($CDCl_3$, 400 MHz) for the cycloaddition reaction of epichlorohydrin using CO_2 and N_2 gases with pressure ratio of 4/4 (total of 8 bar) and MOF**1** as a catalyst (Table 1, entry no. 6).
25. **Figure S20.** ^{1}H NMR ($CDCl_3$, 400 MHz) spectra for the cycloaddition reaction of epichlorohydrin using CO_2 and N_2 gases with pressure ratio of 6/2 (total of 8 bar) and MOF**1** as a catalyst (Table 1, entry no. 7).
26. **Figure S21.** ^{1}H NMR ($CDCl_3$, 400 MHz) spectra for the cycloaddition reaction of epichlorohydrin using mixed gas (CO_2:N_2) with ratio of 13:87% catalyzed by MOF**1** (Table 1, entry no. 8).
27. **Figure S22.** ^{1}H NMR ($CDCl_3$, 400 MHz) spectra for the cycloaddition reaction of propylene oxide with CO_2 catalyzed by MOF**1** (Table 2, entry no. 2).

28. **Figure S23.** ^{1}H NMR ($CDCl_3$, 400 MHz) spectra for the cycloaddition reaction of butylene oxide with CO_2 catalyzed by MOF**1** (Table 2, entry no. 3).
29. **Figure S24.** ^{1}H NMR ($CDCl_3$, 400 MHz) spectra for the cycloaddition reaction of 1,2-epoxyhexane with CO_2 catalyzed by MOF**1** (Table 2, entry no. 4).
30. **Figure S25.** ^{1}H NMR ($CDCl_3$, 400 MHz) spectra for the cycloaddition reaction of 1,2-epoxydecane with CO_2 catalyzed by MOF**1** (Table 2, entry no. 5).
31. **Figure S26.** ^{1}H NMR ($CDCl_3$, 400 MHz) spectra for the cycloaddition reaction of butyl glycidyl ether with CO_2 catalyzed by MOF**1** (Table 2, entry no. 6).
32. **Figure S27.** ^{1}H NMR ($CDCl_3$, 400 MHz) spectra for the cycloaddition reaction of allyl glycidyl ether with CO_2 catalyzed by MOF**1** (Table 2, entry no. 7).
33. **Figure S28.** ^{1}H NMR ($CDCl_3$, 400 MHz) spectra for the cycloaddition reaction of styrene oxide with CO_2 catalyzed by MOF**1** (Table 2, entry no. 8).
34. **Figure S29.** ^{1}H NMR ($CDCl_3$, 400 MHz) spectra for the cycloaddition reaction of *p*-chloro styrene oxide with CO_2 catalyzed by MOF**1** (Table 2, entry no. 9).
35. **Figure S30.** ^{1}H NMR ($CDCl_3$, 400 MHz) spectra for the cycloaddition reaction of phenyl glycidyl ether with CO_2 catalyzed by MOF**1** (Table 2, entry no. 10).
36. **Table S5.** Comparison table for various previously reported MOFs where Co-catalyst free CO_2 conversion is carried out.
37. **Figure S31.** Leaching test for **MOF1**.
38. **Figure S32.** PXRD patterns of MOF**1** (a) pattern calculated from single crystal X- ray data, (b) as-synthesized sample before heating, (c) activated sample by heating at 150 ^{o}C for 20 hours, (d) sample recovered after five catalytic cycles.
39. **Figure S33.** FT-IR spectra for MOF**1** and **2**, and their recovered samples after catalysis.

40. **Figure S34.** SEM image of MOF**1** recovered after catalysis which shows that the morphology is retained after the catalysis and confirms that catalyst is stable.
41. **Figure S35.** Optimized structures of $TATAB^{3-}$ ligand with a $\{Co_2(OOC)_4(H_2O)\}$ SBU with various epoxides showing the coordination of epoxides with Lewis acidic Co(II) center. Atom colors: Co-green; C-dark grey; O-Red; H-white and N-blue.
42. **Table S6.** Co-ordinates for the optimized structure of MOF and MOF with CO_2.
43. **Table S7.** Co-ordinates for the optimized structure of MOF with different epoxides.

X-ray Crystallography

Single crystal X-ray structural data of MOFs **1** and **2** were collected on a CMOS based Bruker D8 Venture PHOTON 100 diffractometer equipped with a INCOATEC micro-focus source with graphite monochromated Mo Kα radiation (λ = 0.71073 Å) operating at 50 kV and 30 mA. The SAINT[1] program was used for integration of diffraction profiles and absorption correction was made with SADABS program.[2] The structures were initially solved by SIR 92[3] and refined by full matrix least square method using SHELXL-2013[4] and WinGX system, Ver 2013.3.[5] The non hydrogen atoms in all the structures were located from the difference Fourier map and refined anisotropically. All the hydrogen atoms were fixed by HFIX and placed in ideal positions and included in the refinement process using riding model with isotropic thermal parameters. The disordered guest solvent molecules in MOFs **1** and **2** were treated with SQUEEZE option of PLATON[6] multipurpose crystallographic software. The potential solvent accessible area or void space was calculated using the PLATON[21] software. All the crystallographic and structure refinement data of the MOFs **1** and **2** is summarized in Table1. Selected bond lengths, angles and hydrogen bond details of **1** and **2** are summarized in Tables S1 and S2 respectively. The

crystallographic information files are deposited with the CCDC numbers 1836675 and 1836674 for MOFs **1** and **2** respectively.

Table S1. Crystal data and structure refinement parameters for MOF**1** and **2**.

Parameters	**MOF1**	**MOF2**
Empirical formula	$C_{114}H_{102}O_{27}N_{30}Co_6$	$C_{114}H_{102}O_{27}N_{30}Ni_6$
Formula mass	2677.81	2676.37
Crystal system	Cubic	Cubic
Space group	*Im-3*(No.204)	*Im-3*(No.204)
a /Å	28.412(6)	28.282(4)
b /Å	28.412(6)	28.282(4)
c /Å	28.412(6)	28.282(4)
α (°)	90.00	90.00
β (°)	90.00	90.00
γ(°)	90.00	90.00
V(Å^3)	22935.4(8)	22622(6)
Z	12	12
ρ(g cm^{-3})	0.758	0.768
μ(mm^{-1})	0.468	0.534
F(000)	5340	5364
T(K)	120	120
λ(Mo K$_\alpha$)(Å)	0.71073	0.71073
Θ_{min}(°)	2.3	2.3
Θ_{max}(°)	25.0	25.0
Total data	28647	27365
Unique data	3597	3550
R_{int}	0.057	0.051
Data [I>2σ(I)]	2798	2674
[a]R_1	0.1015	0.1002
[b]wR_2	0.3230	0.3159
S	1.33	1.28
CCDC numbers	1836675	1836674

[a]$R_1 = \sum \| F_0 | - | F_c \| / \sum | F_o |$, [b]$wR_2 = [\sum w(F_o^2-F_c^2)^2/\sum w(Fo^2)^2]^{1/2}$

Table S2. Selected bond lengths (Å) and angles (°) for MOF**1**.

Bond lengths (Å) and Bond angles (°)			
Co1-O1	2.002(4)	$O1^{i}$-Co1-N4	95.27(12)
Co1-N4	2.116(6)	$O1^{ii}$-Co1-N4	95.27(12)
Co1-$O1^{i}$	2.002(4)	$O1^{iii}$-Co1-N4	95.27(12)
Co1-$O1^{ii}$	2.002(4)	$O1^{i}$-Co1-$O1^{ii}$	90.20(17)
Co1-$O1^{iii}$	2.002(4)	$O1^{i}$-Co1-$O1^{iii}$	88.83(17)
Co2-O1W	1.985(11)	$O1^{ii}$-Co1-$O1^{iii}$	169.46(17)
Co2-O2	2.031(3)	O1W-Co2-O2	96.74(10)
Co2-$O2^{i}$	2.031(3)	O1W-Co2-$O2^{i}$	96.74(10)
Co2-$O2^{ii}$	2.031(3)	O1W-Co2-$O2^{ii}$	96.74(10)
Co2-$O2^{iii}$	2.031(3)	O1W-Co2-$O2^{iii}$	96.74(10)
		O2-Co2-$O2^{i}$	166.52(16)
		O2-Co2-$O2^{ii}$	87.29(14)
O1-Co1-N4	95.27(12)	O2-Co2-$O2^{iii}$	91.14(14)
O1-Co1-$O1^{i}$	169.46(17)	$O2^{i}$-Co2-$O2^{ii}$	91.14(14)
O1-Co1-$O1^{ii}$	88.83(17)	$O2^{i}$-Co2-$O2^{iii}$	87.29(14)
O1-Co1-$O1^{iii}$	90.20(17)	$O2^{ii}$Co2-$O2^{iii}$	166.52(16)

Symmetry codes : (i) x,-y,1-z; (ii) x,y,1-z; (iii) x,-y, z.

Table S3. Selected bond lengths (Å) and angles (°) for MOF**2**.

Bond lengths (Å) and Bond angles (°)			
Ni1-O1	2.007(3)	$O1^{i}$-Ni1-O1W	95.91(10)
Ni1-O1W	2.028(11)	$O1^{ii}$-Ni1-O1W	95.91(10)
Ni1-$O1^{i}$	2.007(3)	$O1^{iii}$-Ni1-O1W	95.91(10)
Ni1-$O1^{ii}$	2.007(3)	$O1^{i}$-Ni1-$O1^{ii}$	88.63(14)
Ni1-$O1^{iii}$	2.007(3)	$O1^{i}$-Ni1-$O1^{iii}$	90.15(14)
Ni2-O2	1.983(4)	$O1^{ii}$-Ni1-$O1^{iii}$	168.18(15)
Ni2-N3	2.055(6)	O2-Ni2-N3	95.39(11)
Ni2-$O2^{i}$	1.983(4)	O2-Ni2-$O2^{i}$	169..23(16)
Ni2-$O2^{ii}$	1.983(4)	O2-Ni2-$O2^{ii}$	89.70(17)
Ni2-$O2^{iii}$	1.983(4)	O2-Ni2-$O2^{iii}$	89.29(17)
		$O2^{i}$-Ni2-N3	95.39(11)
		$O2^{ii}$-Ni2-N3	95.39(11)
O1-Ni1-O1W	95.91(10)	$O2^{iii}$-Ni2-N3	95.39(11)
O1-Ni1-$O1^{i}$	168.18(15)	$O2^{i}$-Ni2-$O2^{ii}$	89.29(17)
O1-Ni1-$O1^{ii}$	90.15(14)	$O2^{i}$-Ni2-$O2^{iii}$	89.70(17)
O1-Ni1-$O1^{iii}$	88.63(14)	$O2^{ii}$-Ni2-$O2^{iii}$	169.23(16)

Symmetry codes : (i) 1-x,y,-z; (ii) x,y,-z; (iii) 1-x,y,z.

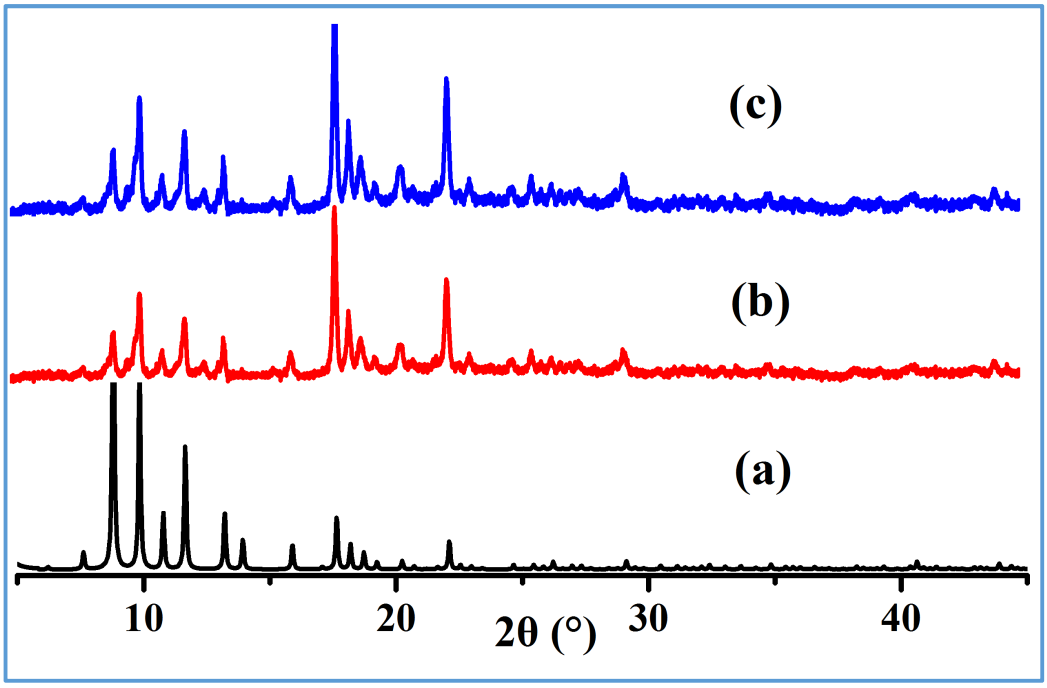

Figure S1. PXRD patterns of MOF**1** (a) pattern calculated from single crystal X-ray data, (b) as-synthesized sample, (c) activated sample by heating at 150 ºC under vacuum for 20 hours.

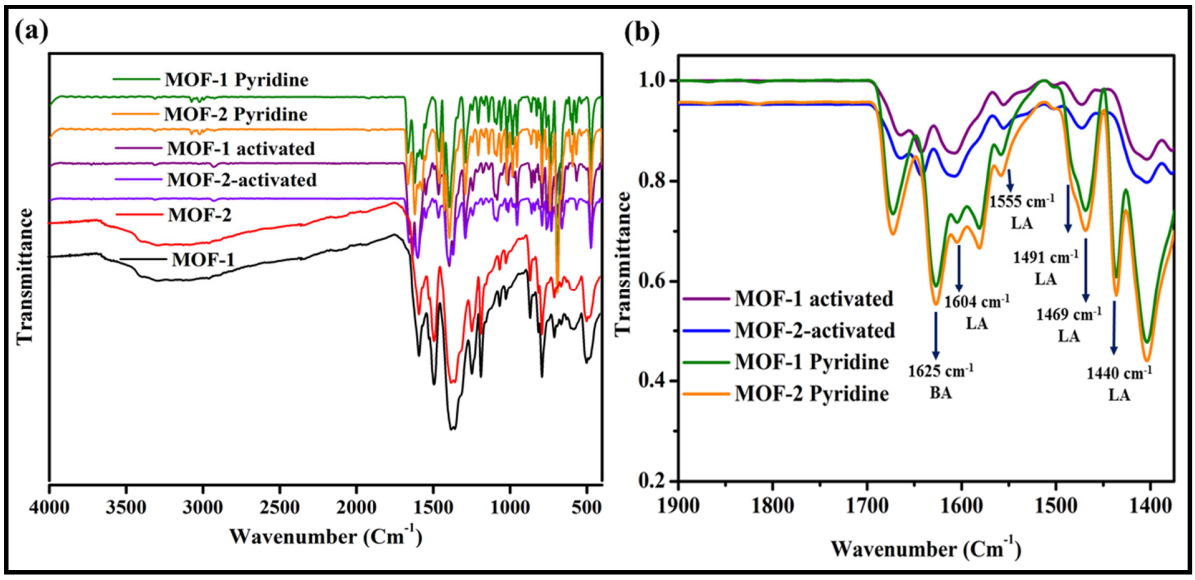

Figure S2. **(a)** FT-IR spectra for MOF**1** and **2**, their activated samples and samples treated with pyridine. (b) Expanded view of the activated MOF1 and MOF2 along with the activated samples treated using pyridine as basic probe for acidic sites.

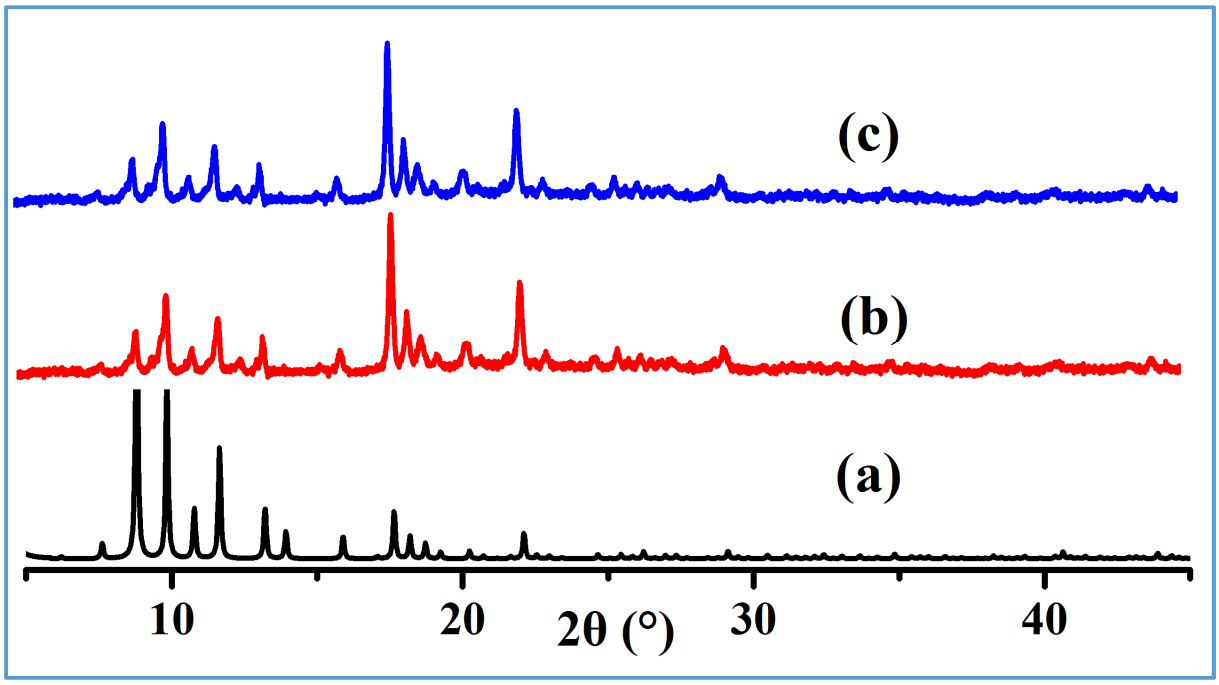

Figure S3. PXRD patterns of MOF**2** (a) pattern calculated from single crystal X- ray data, (b) as-synthesized sample, (c) activated sample by heating at 150 ºC under vacuum for 20 hours.

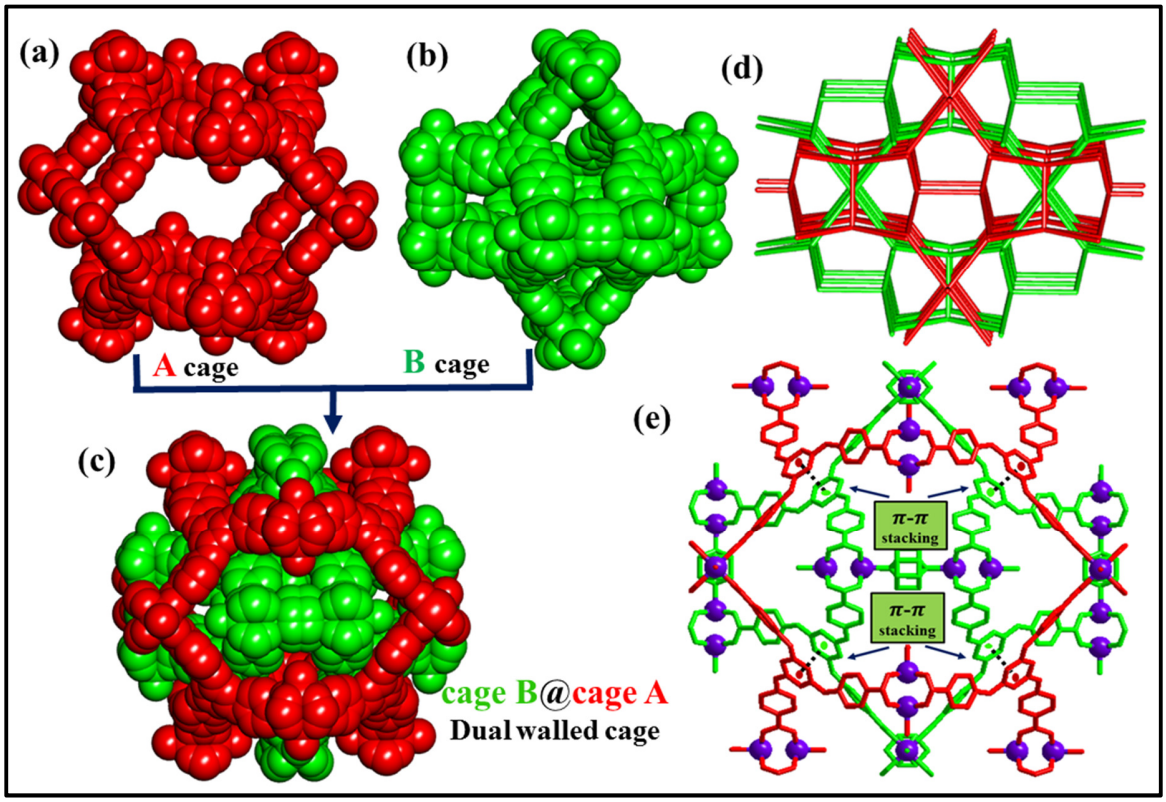

Figure S4. Space-filled view of the cage-A (a), for cage-B (b), and for dual-walled cage formed by encapsulation of cage-B into cage-A (c). (d) TOPOS representation of 3D framework in **1** and **2** with 2-fold interpenetration (two different colors are used to represent two different nets). (e) Π-Π interactions between the two nets with a distance of 3.456 Å.

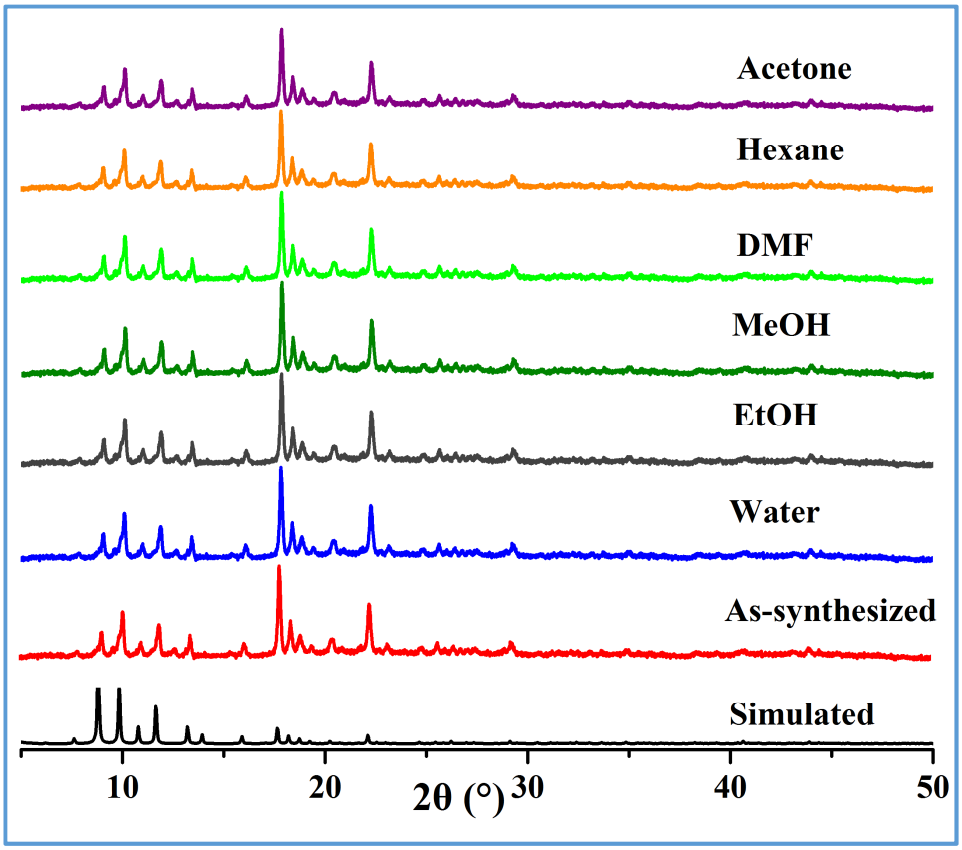

Figure S5. Powder XRD patterns of MOF**1** isolated after treating with different solvents.

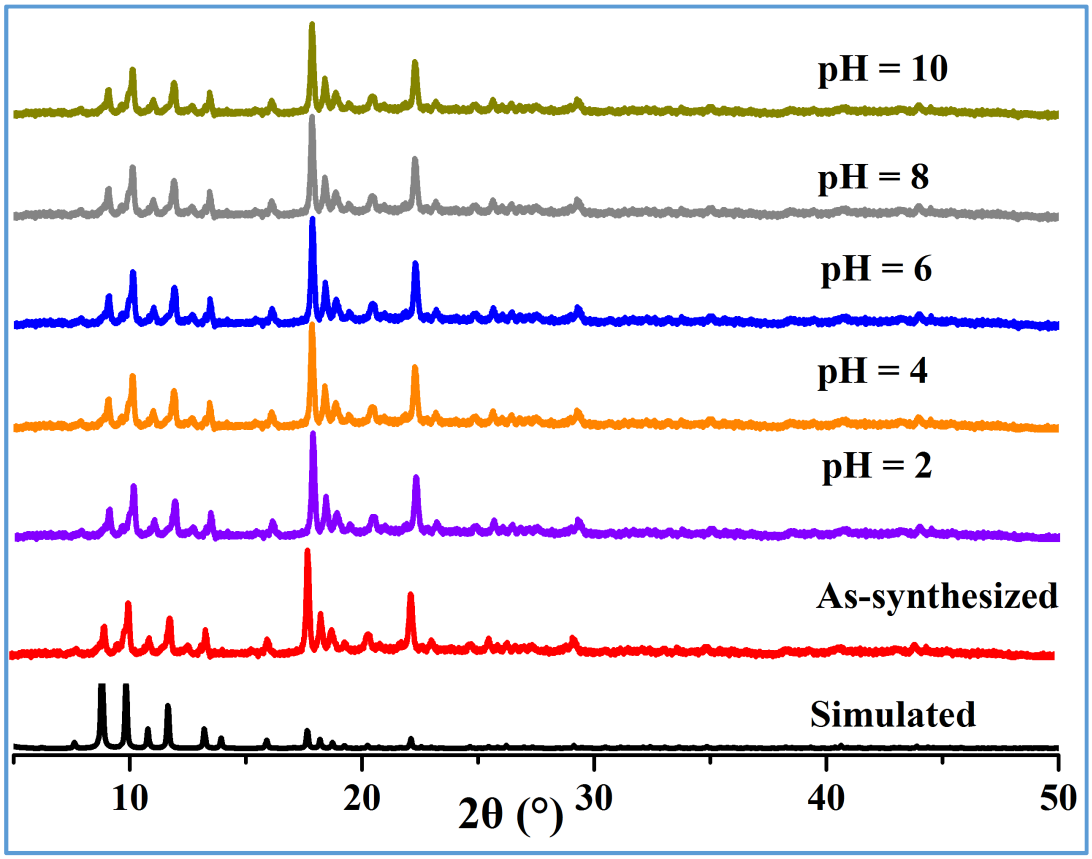

Figure S6. Powder XRD patterns of MOF**1** isolated after treating with different pH conditions.

Gas Adsorption measurements

N_2 isotherm measurements were carried out at 77 K and 273 K also, whereas CO_2 isotherm measurement experiments were conducted at 273 and 298 K using Quadrasorb SI (QUANTACHROME) automatic volumetric instrument. For Ar and H_2 isotherm measurements were conducted at 273K. Ultrapure (99.995%) N_2, He, H_2, Ar and CO_2 gases were used for the isotherm measurements. Before starting isotherm measurements all the sample (~100 mg) was evacuated at 423 K under vacuum (18 mTorr) for 20 hours using Flovac degasser (QUANTACHROME) and purged with ultrapure nitrogen gas on cooling. Then the evacuated sample was introduced to the Quadrasorb SI (QUANTACHROME) automatic volumetric

instrument and further all operations were computer controlled. Dead volume of sample cell was measured using Helium gas (99.995%).

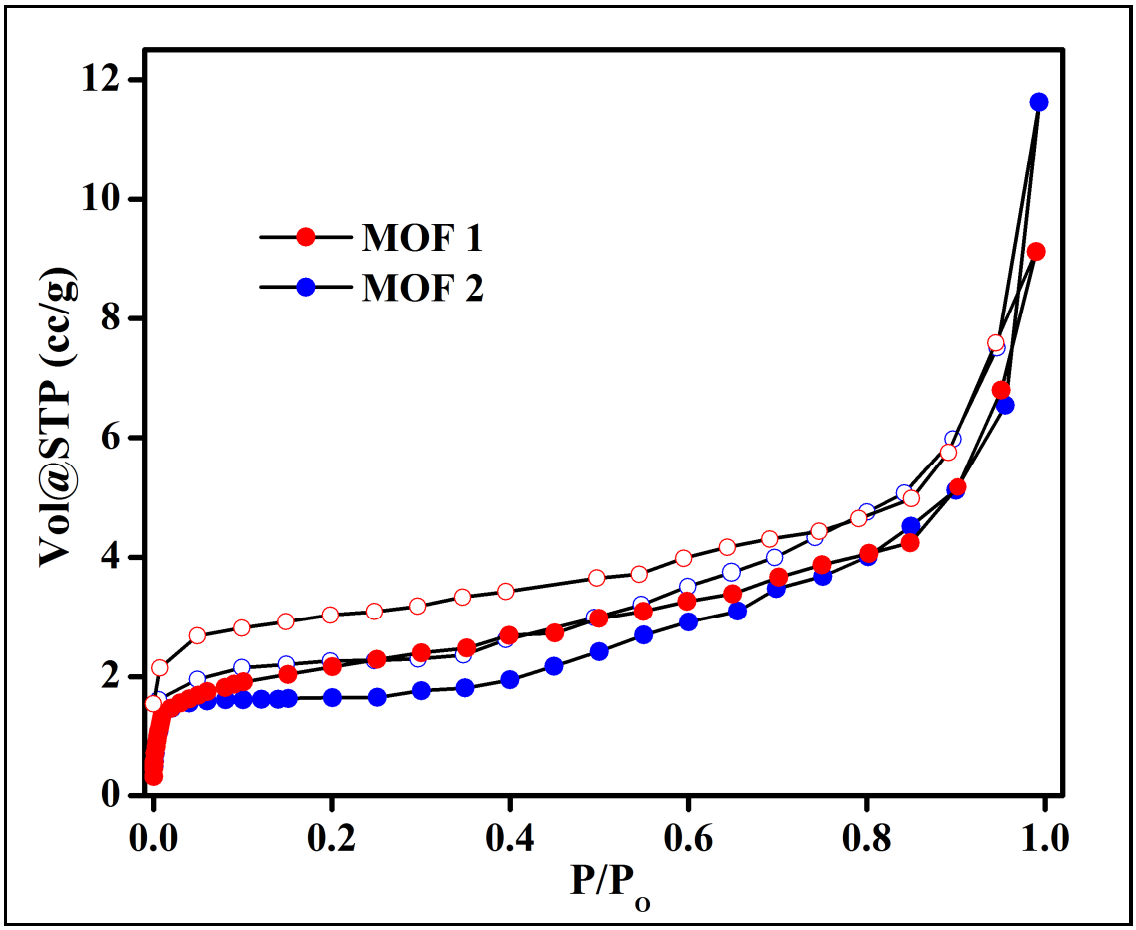

Figure S7. N_2 adsorption-desorption isotherms at 77K for MOF**1**. Closed circles represents adsorption and open circles for desorption.

Analysis of Gas adsorption Isotherms

Clausius-Clapeyron Equation[7] was used to calculate the enthalpies of hydrogen adsorption. By using Langmuir Freundlich equation[8] an accurate fit was retrieved which gives a precise prediction of hydrogen adsorbed at saturation. A modification of Clausius-Clapeyron equation is used for calculations.

$$\ln\left[\frac{P_1}{P_2}\right] = \Delta H_{ads} \; X \left[\frac{T_2 - T_1}{R \; X \; T_2 T_1}\right] \qquad \text{------(i)}$$

where,

P_1 and P_2 = pressures for isotherm at 273K and 298K respectively.

T_1 and T_2 = temperatures for isotherm at 273K and 298K respectively.

ΔH_{ads} = Enthalpy of adsorption.

R = Universal gas constant = 8.314 J/K/mol.

Pressure is a function of amount of gas adsorbed which was determined by using the Langmuir-Freundlich fit.

$$\frac{Q}{Q_m} = \frac{B \; X \; P^{(1/t)}}{1 + (B \; X \; P^{(1/t)})} \qquad \text{------(ii)}$$

where, Q = moles of gas adsorbed.

Q_m = moles of gas adsorbed at saturation.

B and t = constants.

P = Pressure.

By rearranging equation (ii) we get equation (iii)

$$P = \left[\frac{Q/Q_m}{B - (B\ X\ Q/Q_m)}\right]^t \qquad \text{------(iii)}$$

Substituting equation (iii) into equation (i) we get

$$\Delta H_{ads} = \frac{R\ X\ T_1\ X\ T_2}{T_2 - T_1}\ \ln \frac{\left[\frac{Q/Q_{m1}}{B - (B\ X\ Q/Q_{m1})}\right]^{t1}}{\left[\frac{Q/Q_{m2}}{B - (B\ X\ Q/Q_{m2})}\right]^{t2}} \qquad \text{------ (iv)}$$

In equation (iv), subscript 1 and 2 are representing data corresponding to 273K and 298K in case of carbon dioxide gas.

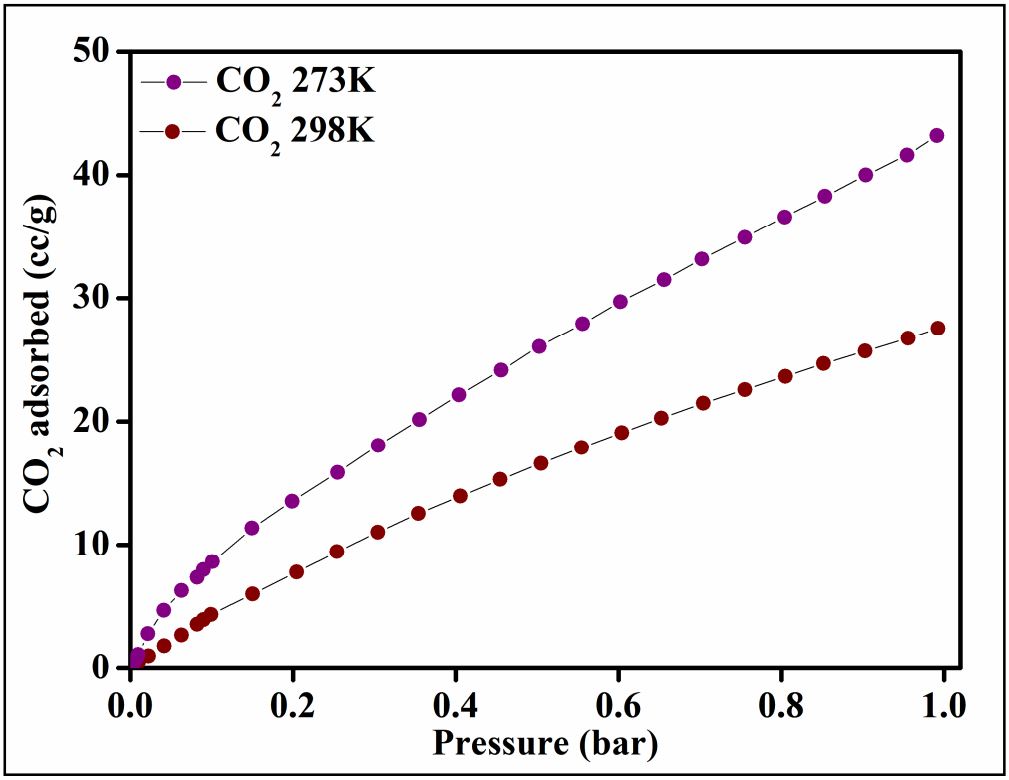

Figure S8. CO_2 adsorption-desorption isotherms carried out at 273 and 298 K for MOF**1**.

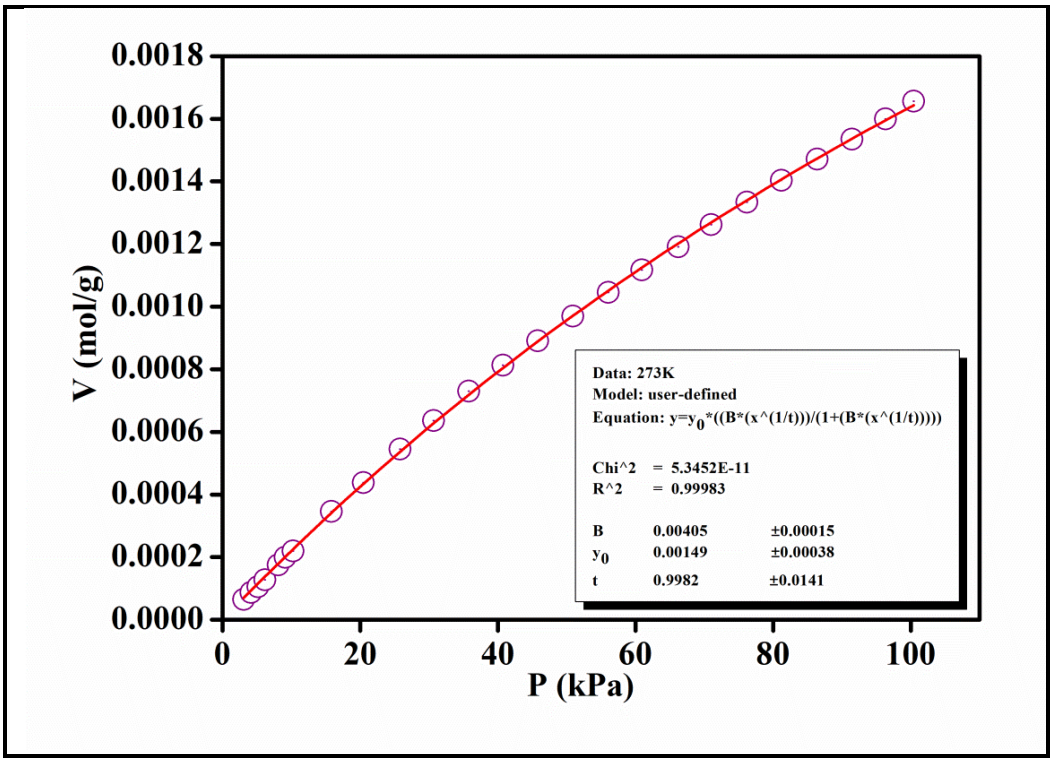

Figure S9. Carbon dioxide adsorption isotherm for MOF**1** at 273 K. The solid line shows the best fit to the data using Langmuir- Freundlich equation.

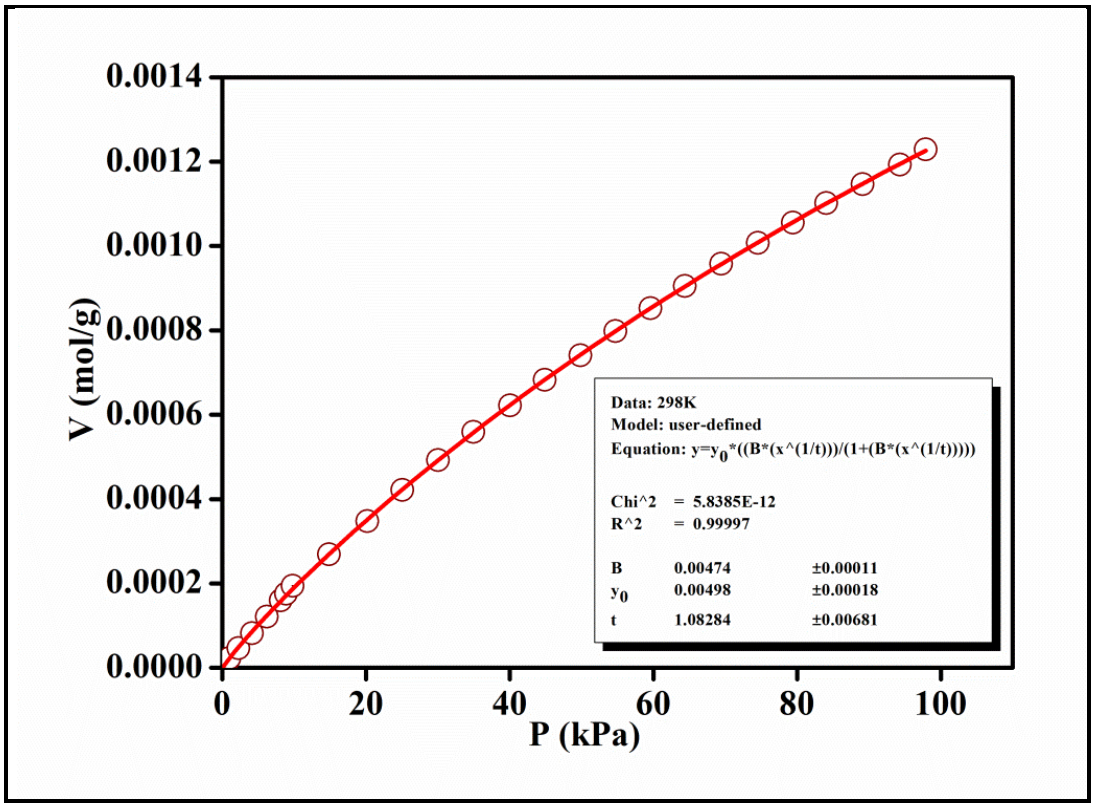

Figure S10. Carbon dioxide adsorption isotherm for MOF**1** at 298 K. The solid line shows the best fit to the data using Langmuir- Freundlich equation.

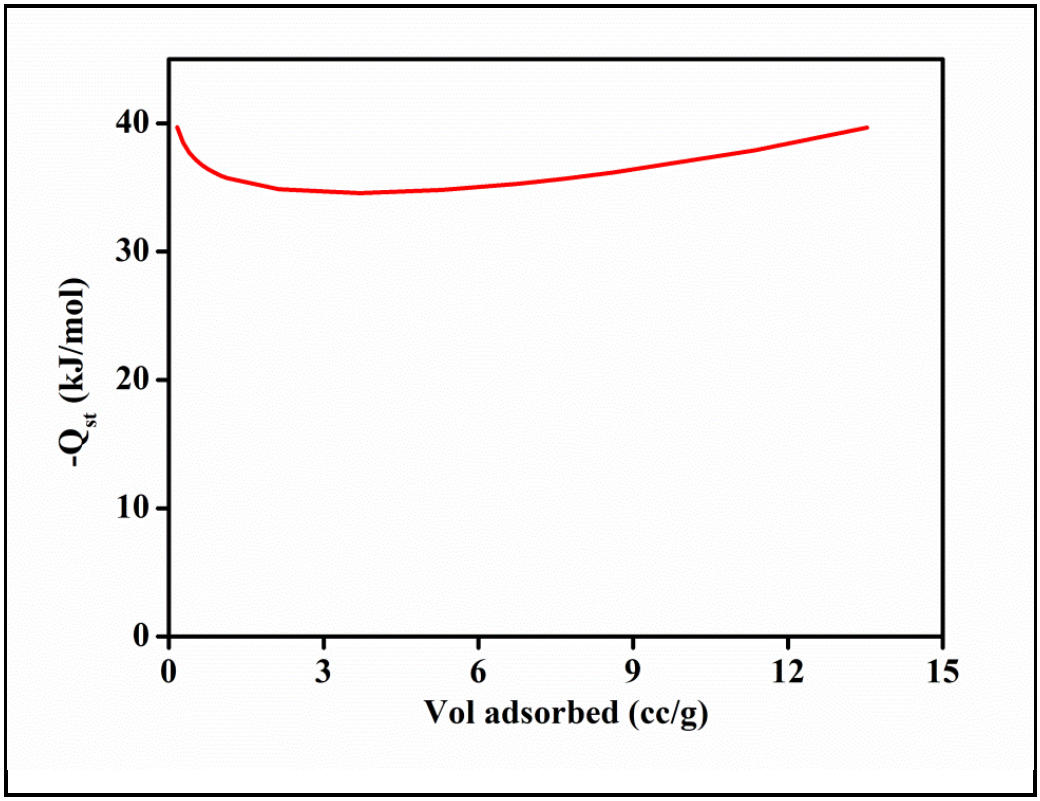

Figure S11. Enthalpy of carbon dioxide adsorption for MOF**1** using Clausius-Clapeyron equation calculations.

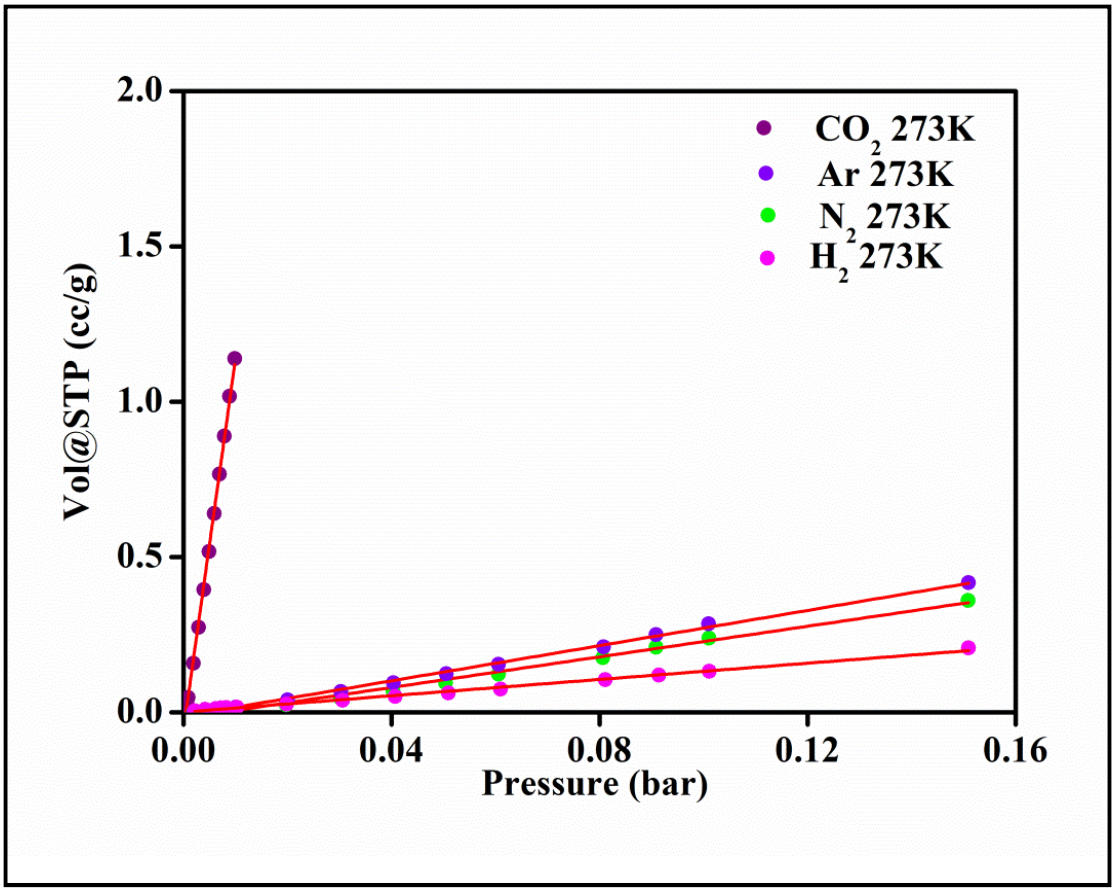

Figure S12. Gas selectivity constants calculated for MOF**1** following the Henry's law from the CO_2, N_2, Ar and H_2 isotherms at 273K.

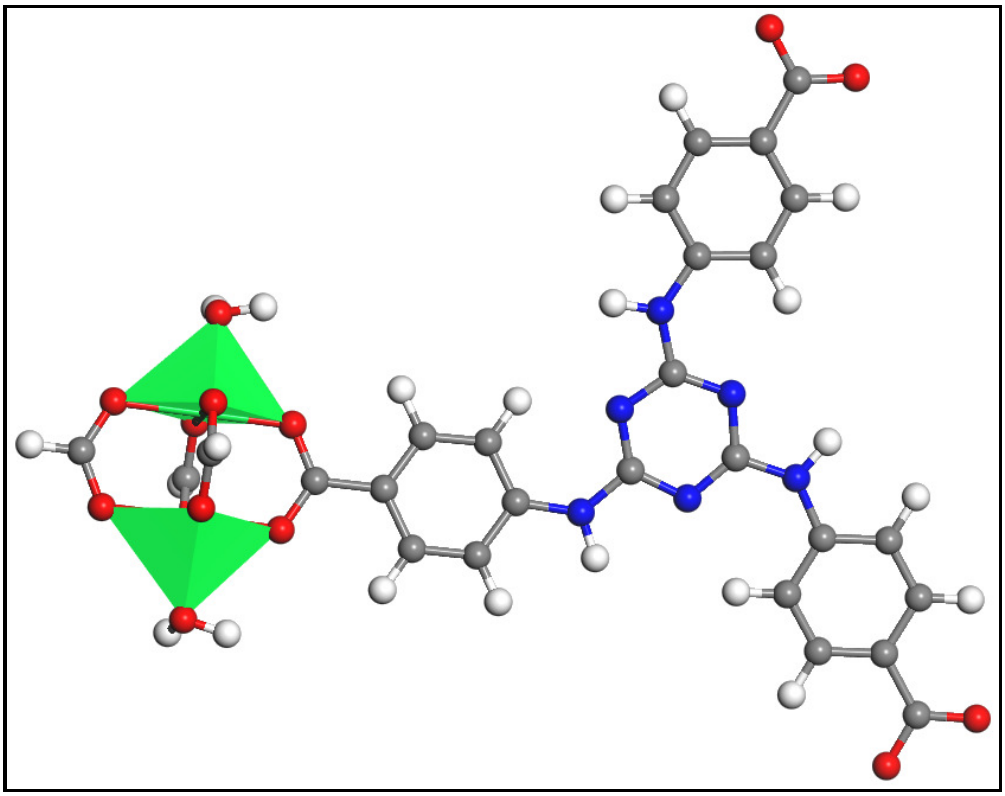

Figure S13. Optimized structure of $TATAB^{3-}$ ligand coordinated to a paddlewheel $Co(OOC)_2(H_2O)_2$ SBU. Atom colors: Co-green; C-dark grey; O-Red; H-white and N-blue.

Table S4. Optimization of reaction parameters for CO_2 cycloaddition with epichlorohydrin.[a]

Entry No.	Catalyst [mol%]	Co-catalyst [mol%]	Pressure [MPa]	Time [h]	Temperature [°C]	Conversion [%][b]
1	None	None	0.1	12	r.t.	0
2	None	None	0.1	12	80	4
3	None	None	0.1	15	80	5
4	MOF**1**	None	0.1	12	r.t.	46
5	MOF**1**	None	0.1	12	80	78
6	MOF**1**	None	0.1	15	80	93
7	MOF**1**	None	0.1	18	80	100
8	MOF**1**	None	0.8	12	80	91
9	MOF**1**	None	0.8	15	80	100

[a]Reaction conditions: Epichlorhydrin (20 mmol), MOF**1** catalyst: (0.2 mol%). [b]The catalytic conversions were determined by ^{1}H NMR analysis using 1,1', 2,2'-tetrachloroethane as internal standard.

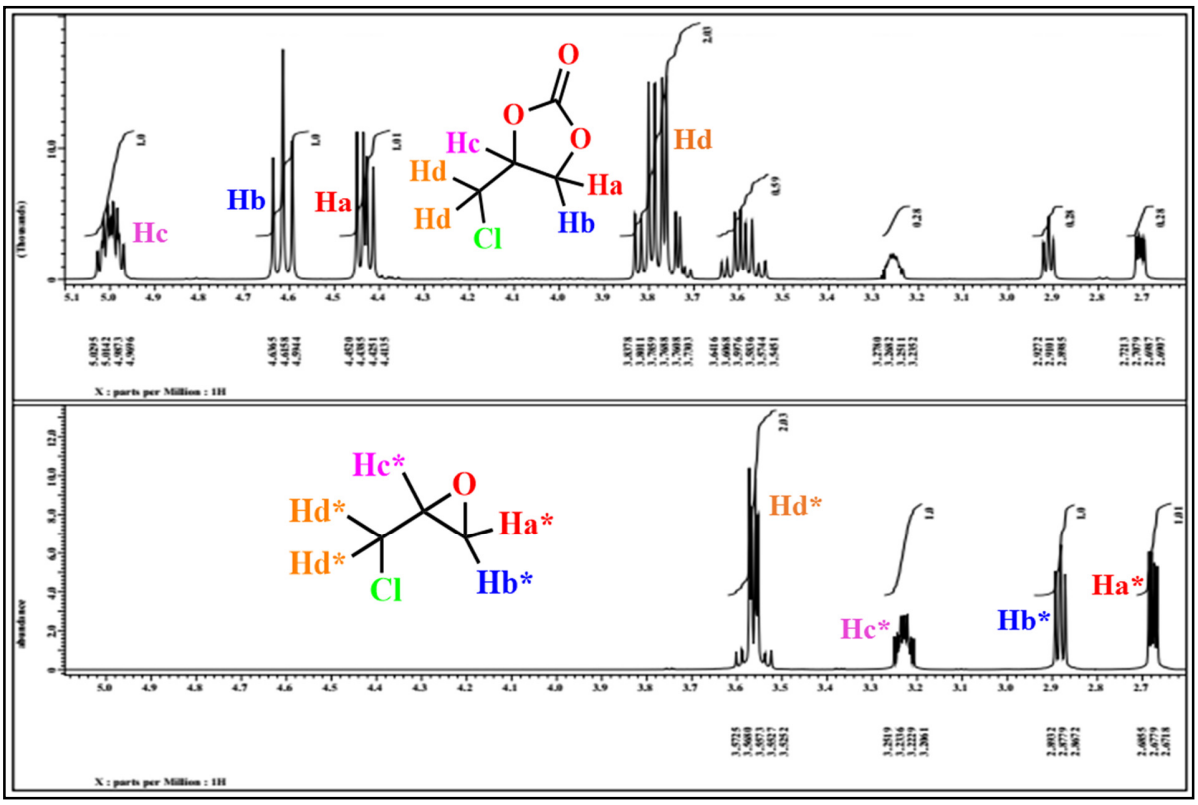

Figure S14. ^{1}H NMR ($CDCl_3$, 400 MHz) spectra for the cycloaddition reaction of epichlorohydrin with CO_2 using MOF**1** as catalyst (Table S4, entry no. 5).

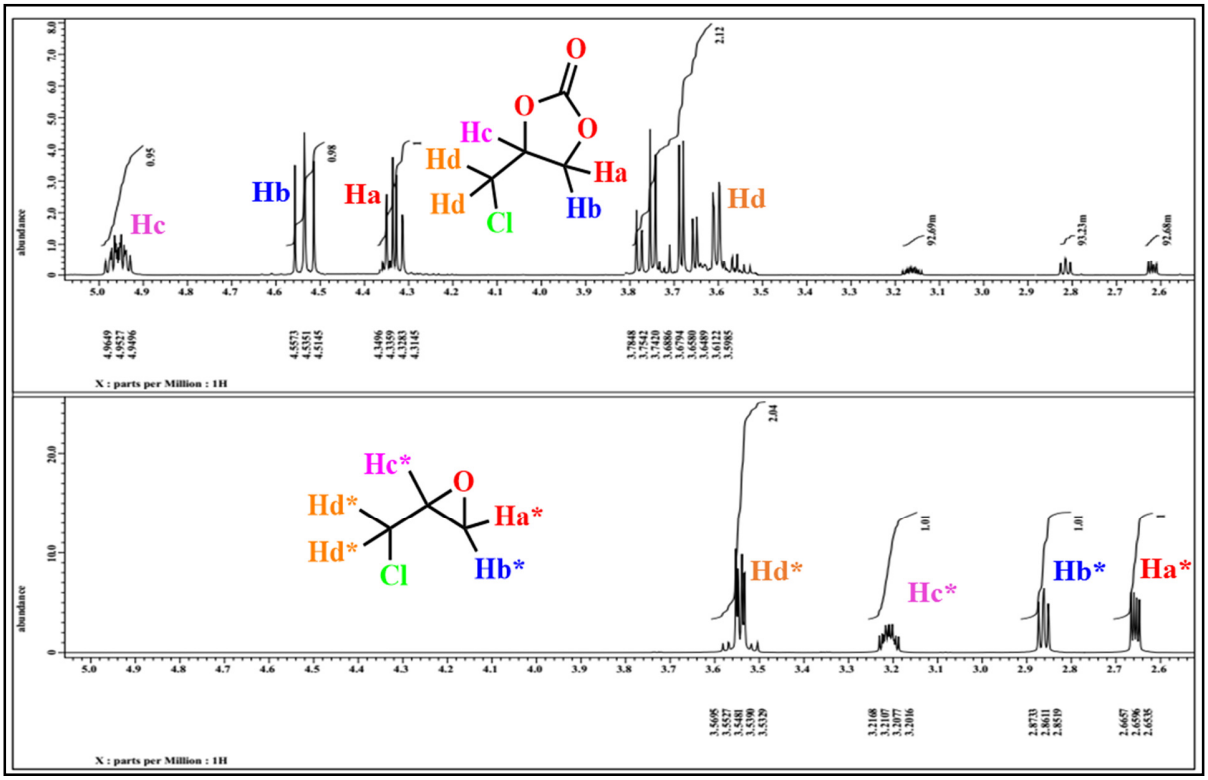

Figure S15. ^{1}H NMR ($CDCl_3$, 400 MHz) spectra for the cycloaddition reaction of epichlorohydrin with CO_2 using MOF**1** as catalyst (Table 1, entry no. 2) & (Table 2, entry no. 1).

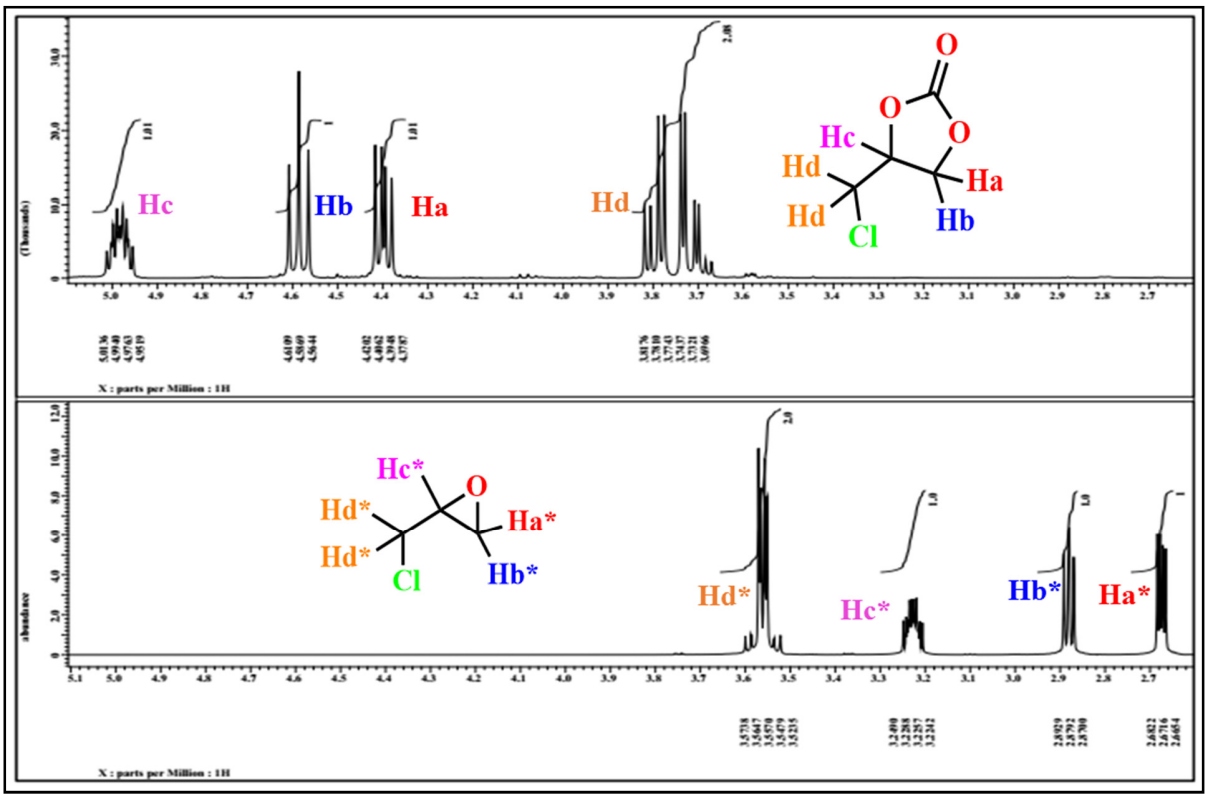

Figure S16. ^{1}H NMR ($CDCl_3$, 400 MHz) spectra for the cycloaddition reaction of epichlorohydrin with CO_2 using MOF**1** as catalyst (Table S4, entry no. 7) & (Table 1, entry no. 4).

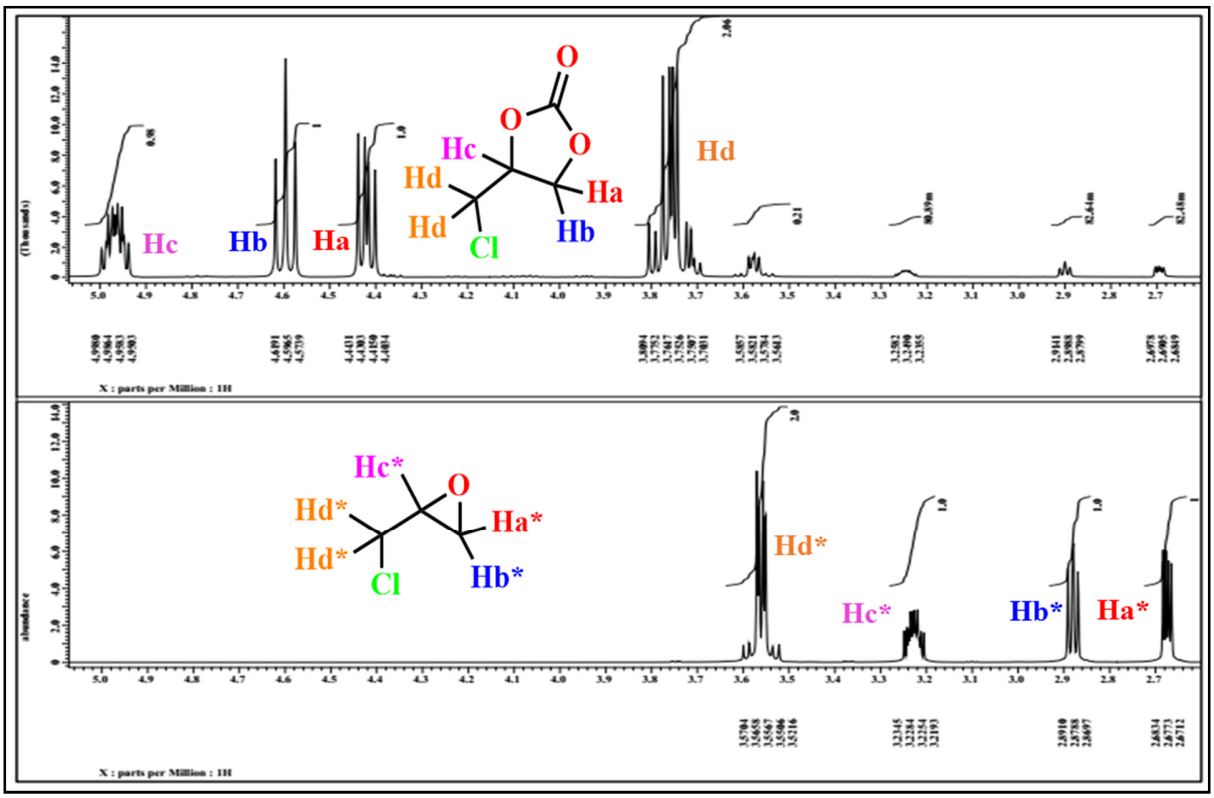

Figure S17. ^{1}H NMR ($CDCl_3$, 400 MHz) spectra for the cycloaddition reaction of epichlorohydrin with CO_2 using MOF**1** as catalyst (Table S4, entry no. 8).

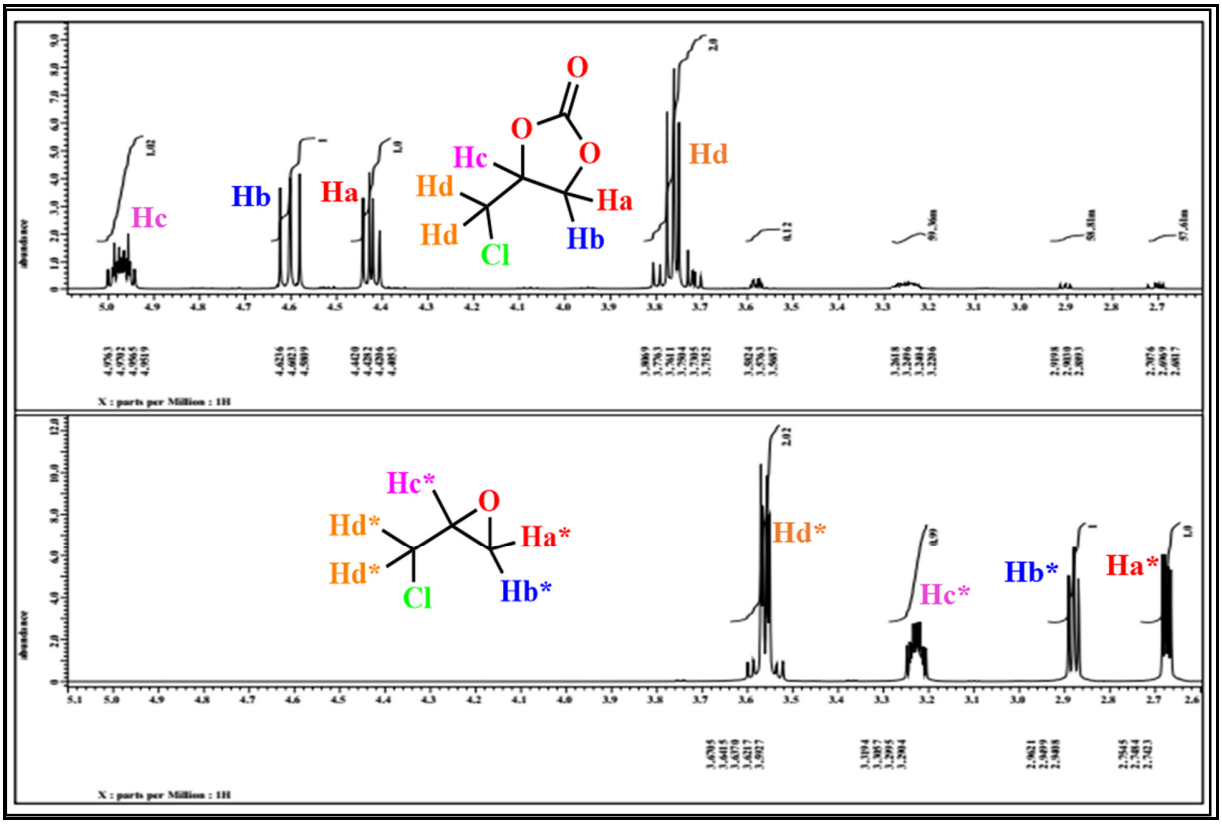

Figure S18. ^{1}H NMR ($CDCl_3$, 400 MHz) spectra for the cycloaddition reaction of epichlorohydrin using CO_2 and N_2 gases with pressure ratio of 2/6 (total of 8 bar) and MOF**1** as a catalyst (Table 1, entry no. 5).

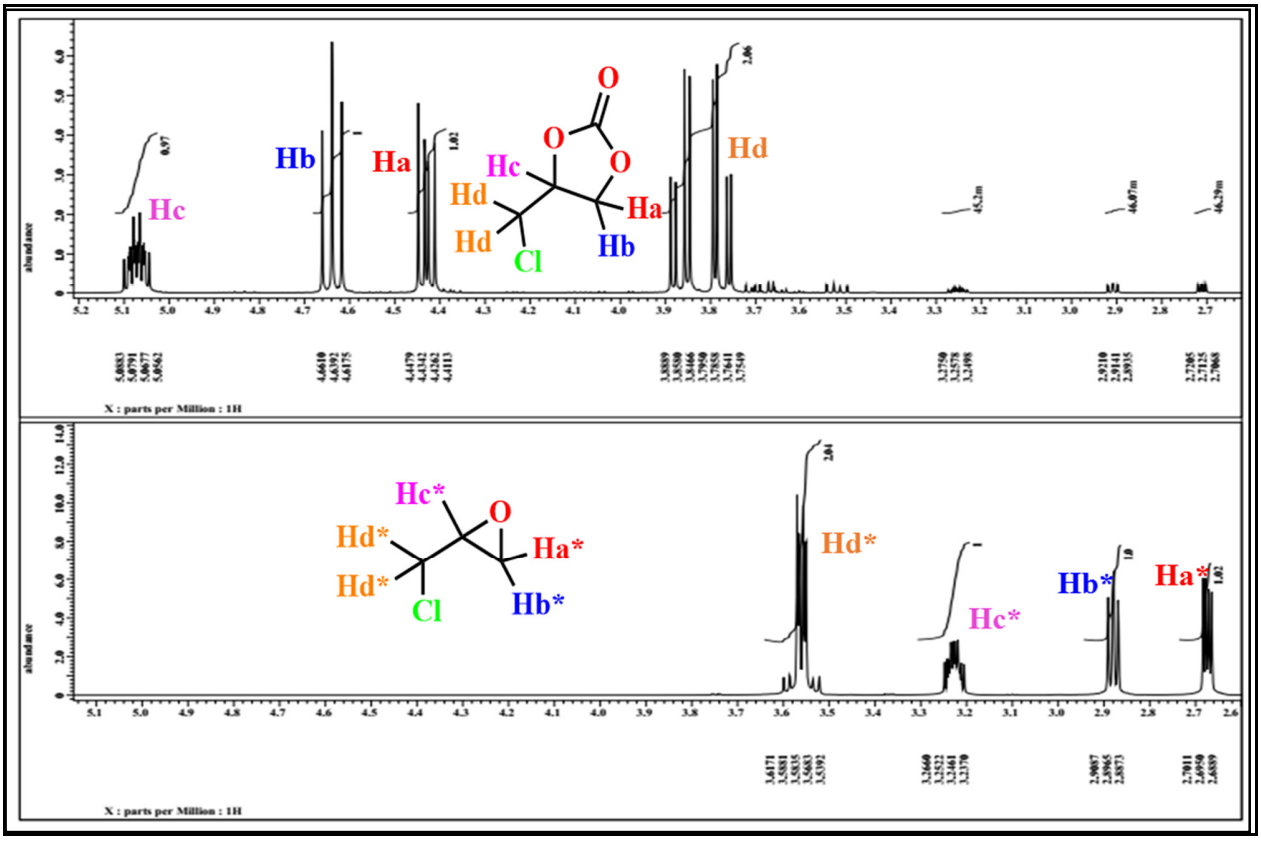

Figure S19. ^{1}H NMR ($CDCl_3$, 400 MHz) for the cycloaddition reaction of epichlorohydrin using CO_2 and N_2 gases with pressure ratio of 4/4 (total of 8 bar) and MOF**1** as a catalyst (Table 1, entry no. 6).

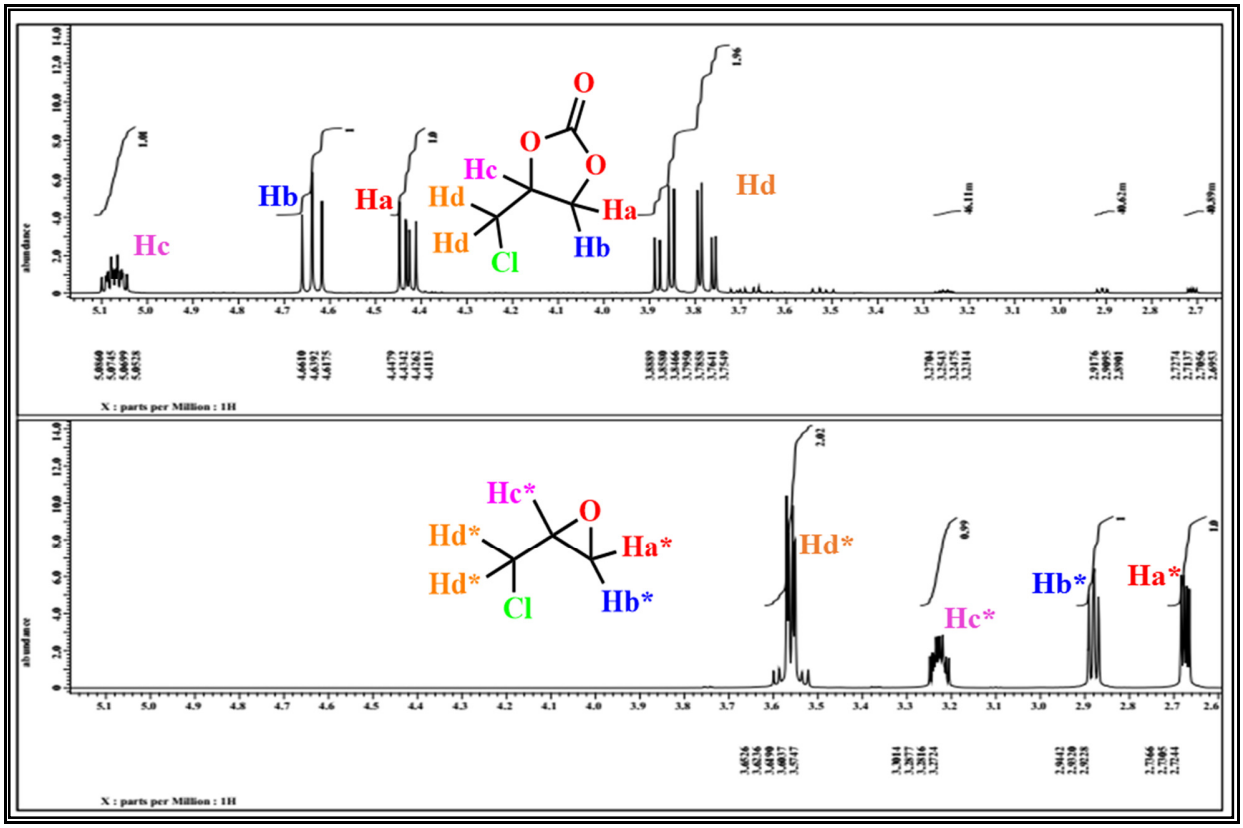

Figure S20. ^{1}H NMR ($CDCl_3$, 400 MHz) spectra for the cycloaddition reaction of epichlorohydrin using CO_2 and N_2 gases with pressure ratio of 6/2 (total of 8 bar) and MOF**1** as a catalyst (Table 1, entry no. 7).

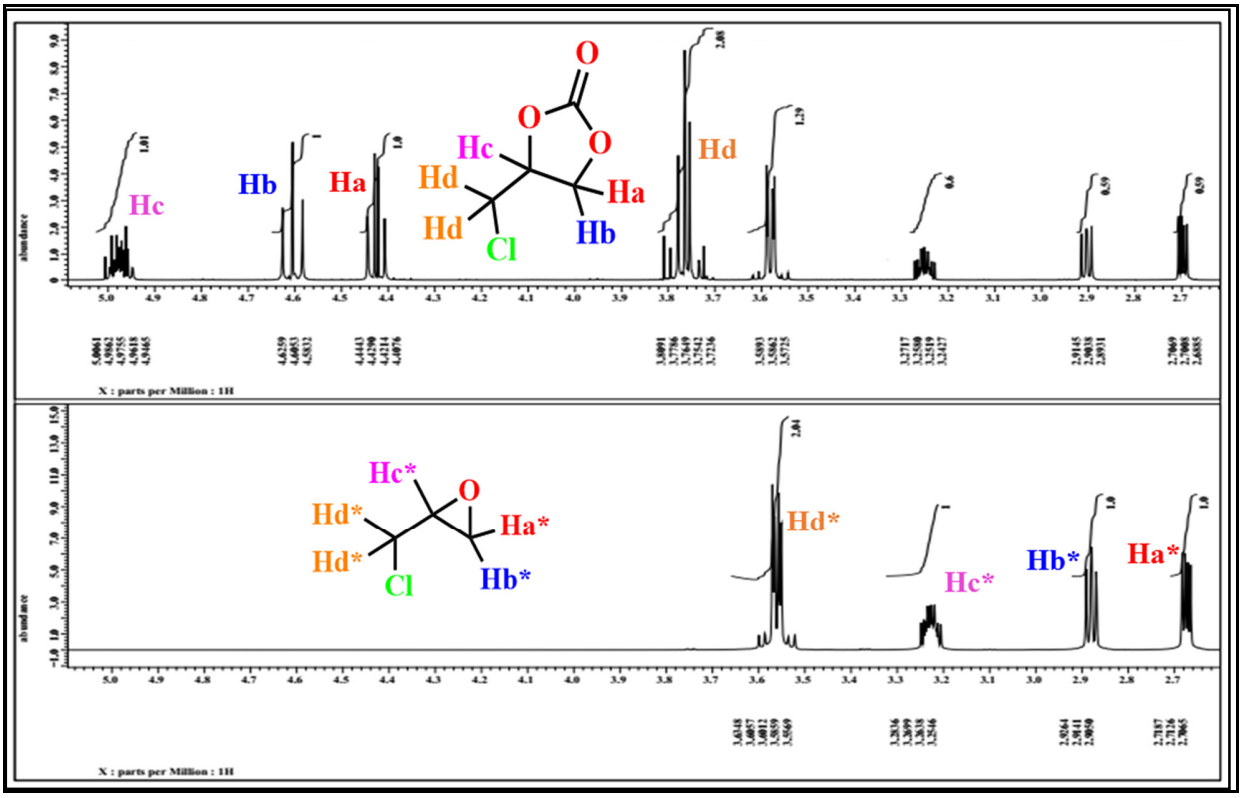

Figure S21. ^{1}H NMR ($CDCl_3$, 400 MHz) spectra for the cycloaddition reaction of epichlorohydrin using mixed gas (CO_2:N_2) with ratio of 13:87% catalyzed by MOF**1** (Table 1, entry no. 8).

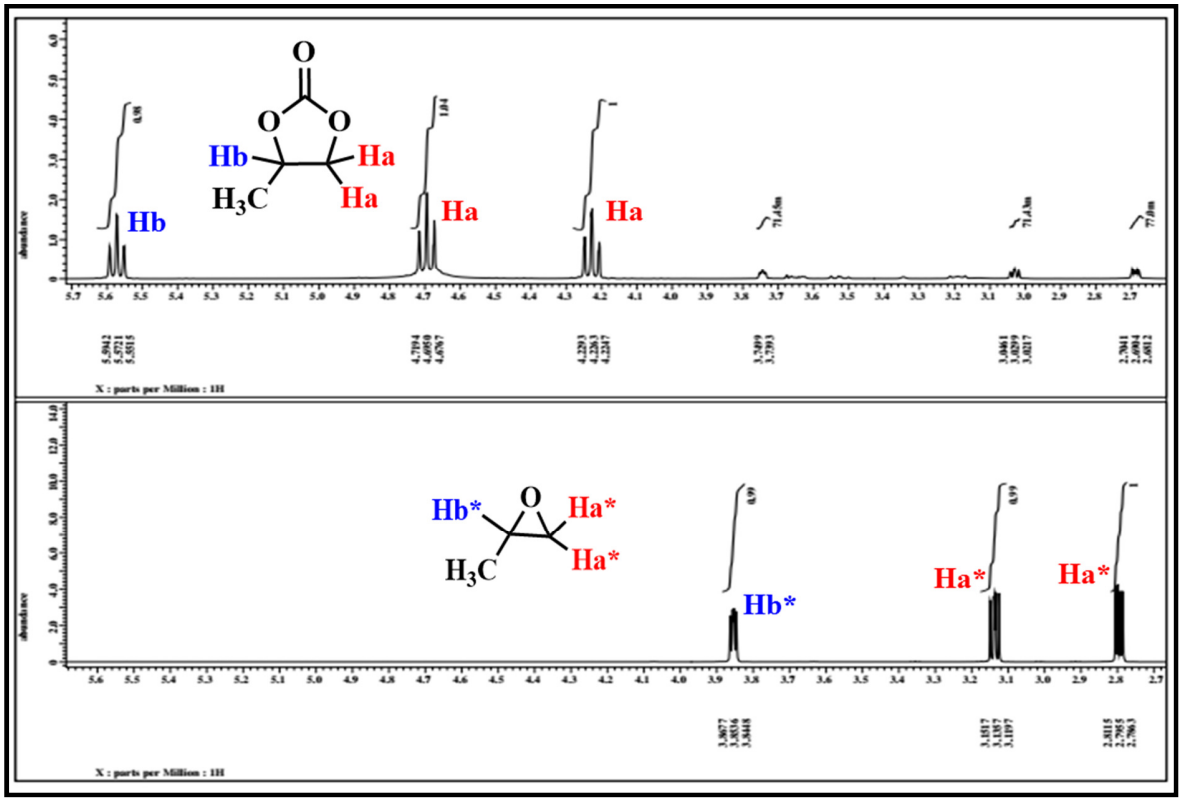

Figure S22. ^{1}H NMR ($CDCl_3$, 400 MHz) spectra for the cycloaddition reaction of propylene oxide with CO_2 catalyzed by MOF**1** (Table 2, entry no. 2).

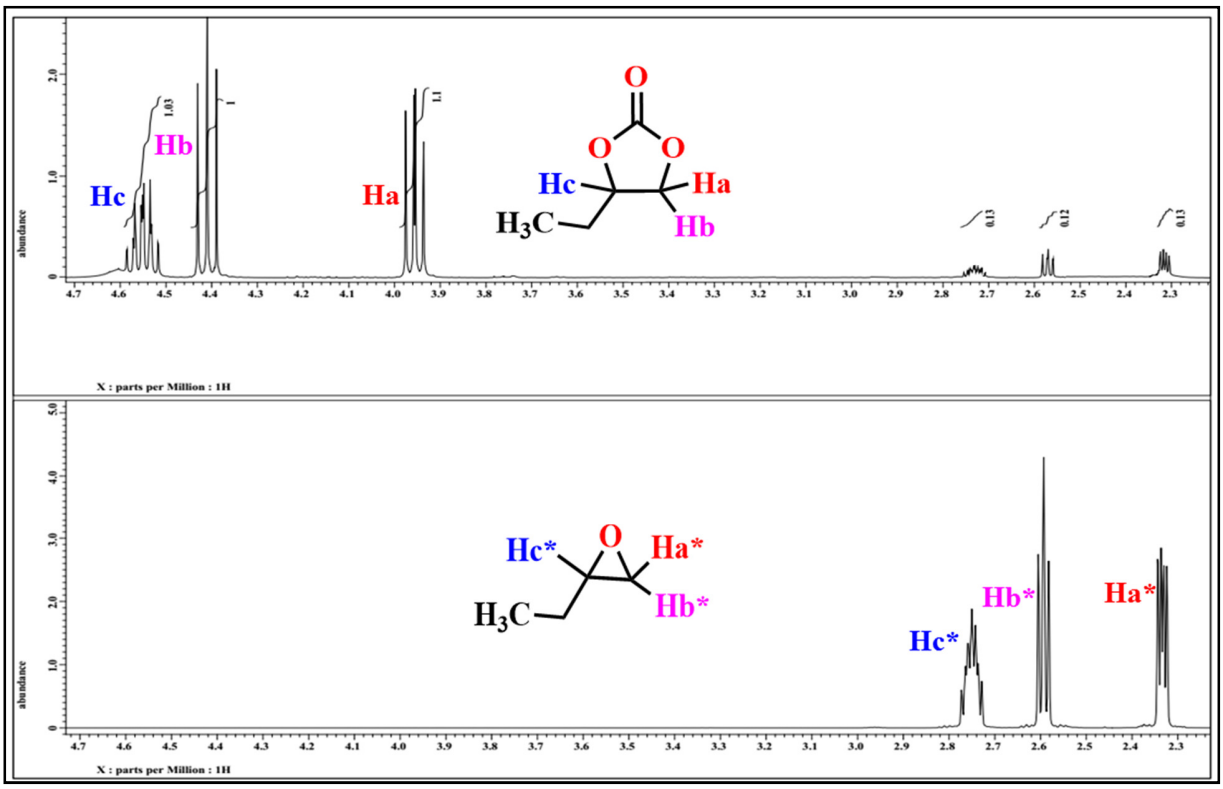

Figure S23. ^{1}H NMR ($CDCl_3$, 400 MHz) spectra for the cycloaddition reaction of butylene oxide with CO_2 catalyzed by MOF**1** (Table 2, entry no. 3).

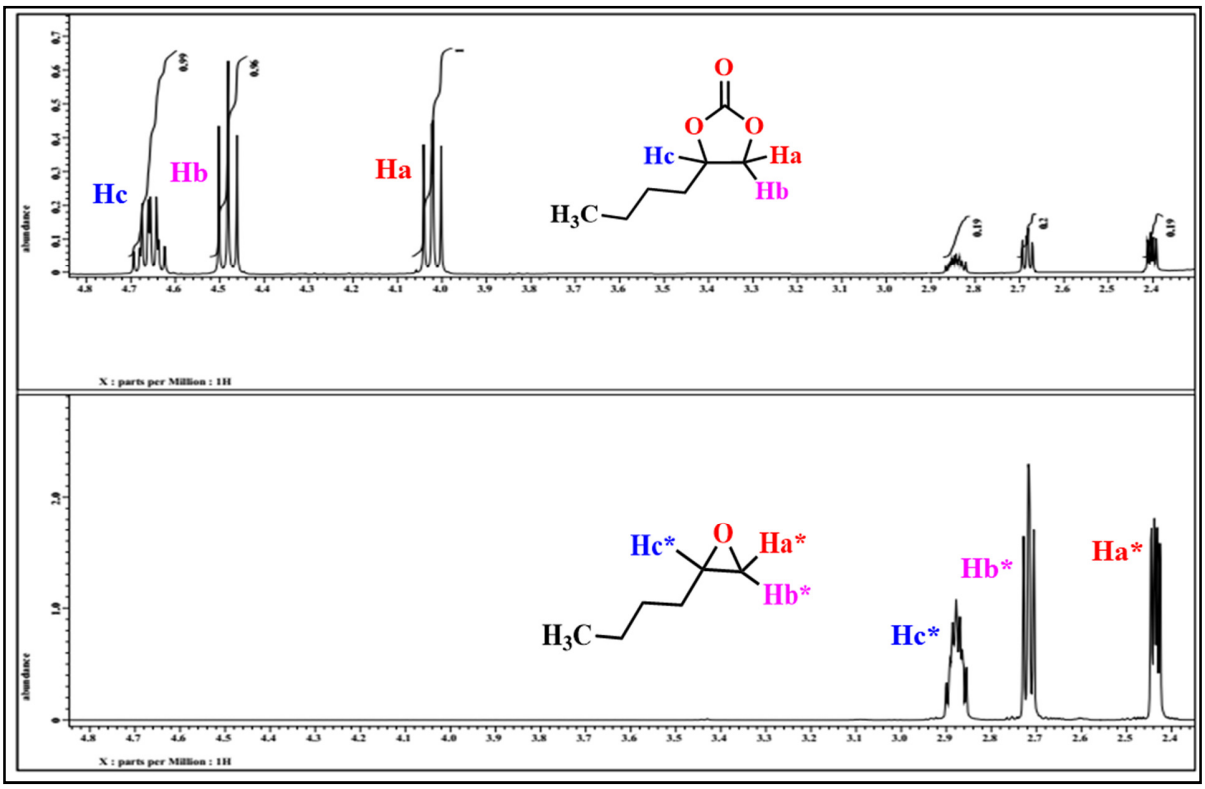

Figure S24. ^{1}H NMR ($CDCl_3$, 400 MHz) spectra for the cycloaddition reaction of 1,2-epoxyhexane with CO_2 catalyzed by MOF**1** (Table 2, entry no. 4).

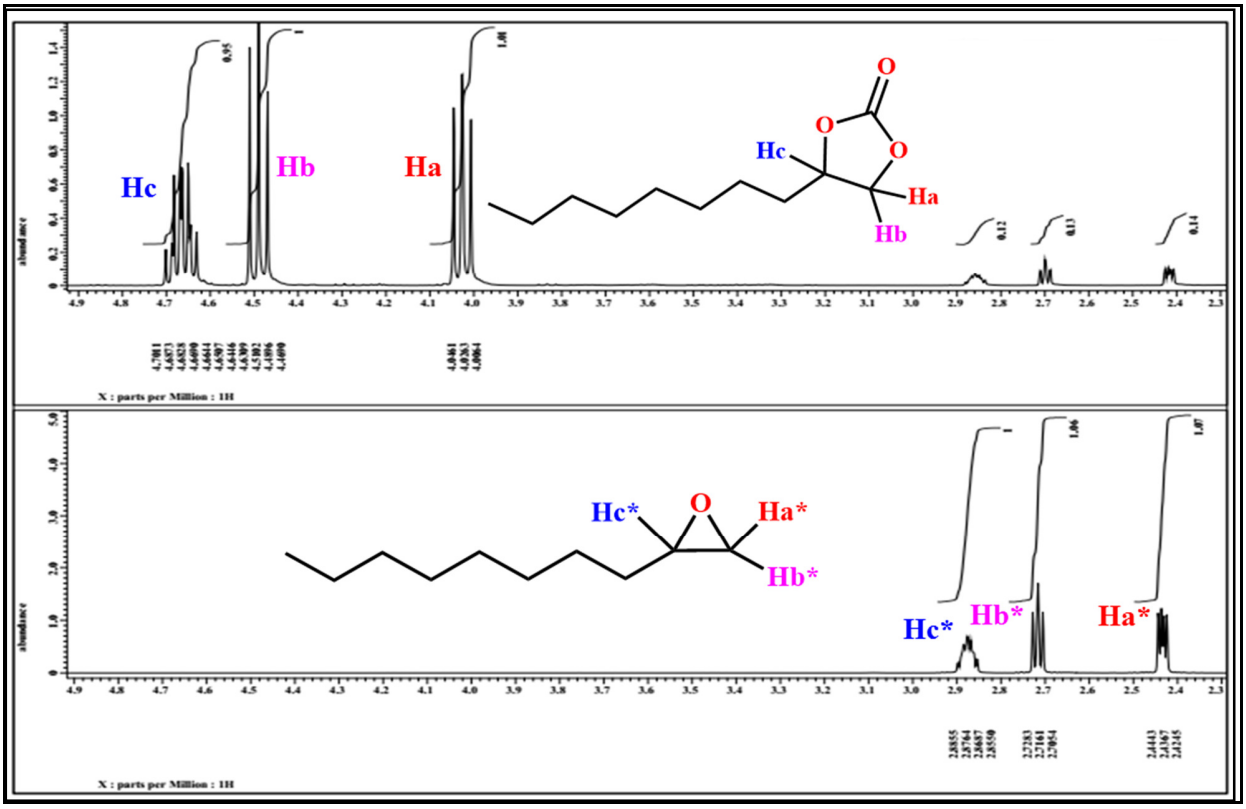

Figure S25. ^{1}H NMR ($CDCl_3$, 400 MHz) spectra for the cycloaddition reaction of 1,2-epoxydecane with CO_2 catalyzed by MOF**1** (Table 2, entry no. 5).

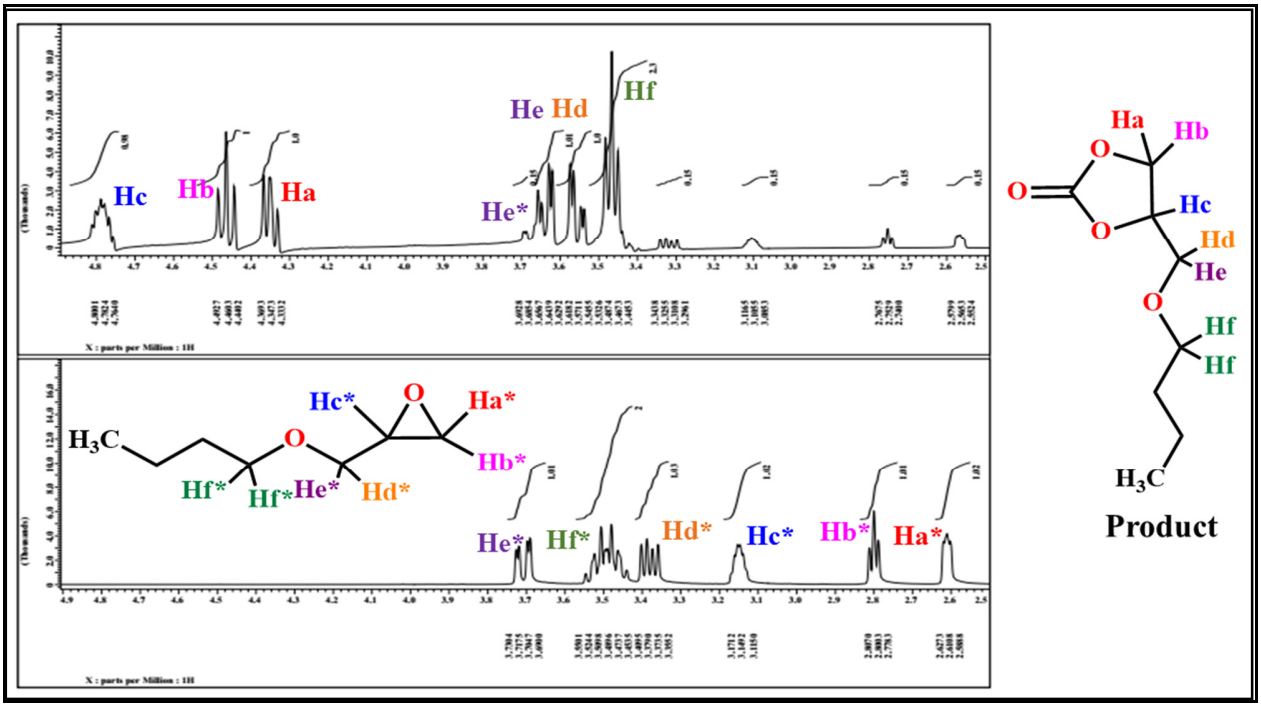

Figure S26. ^{1}H NMR ($CDCl_3$, 400 MHz) spectra for the cycloaddition reaction of butyl glycidyl ether with CO_2 catalyzed by MOF**1** (Table 2, entry no. 6).

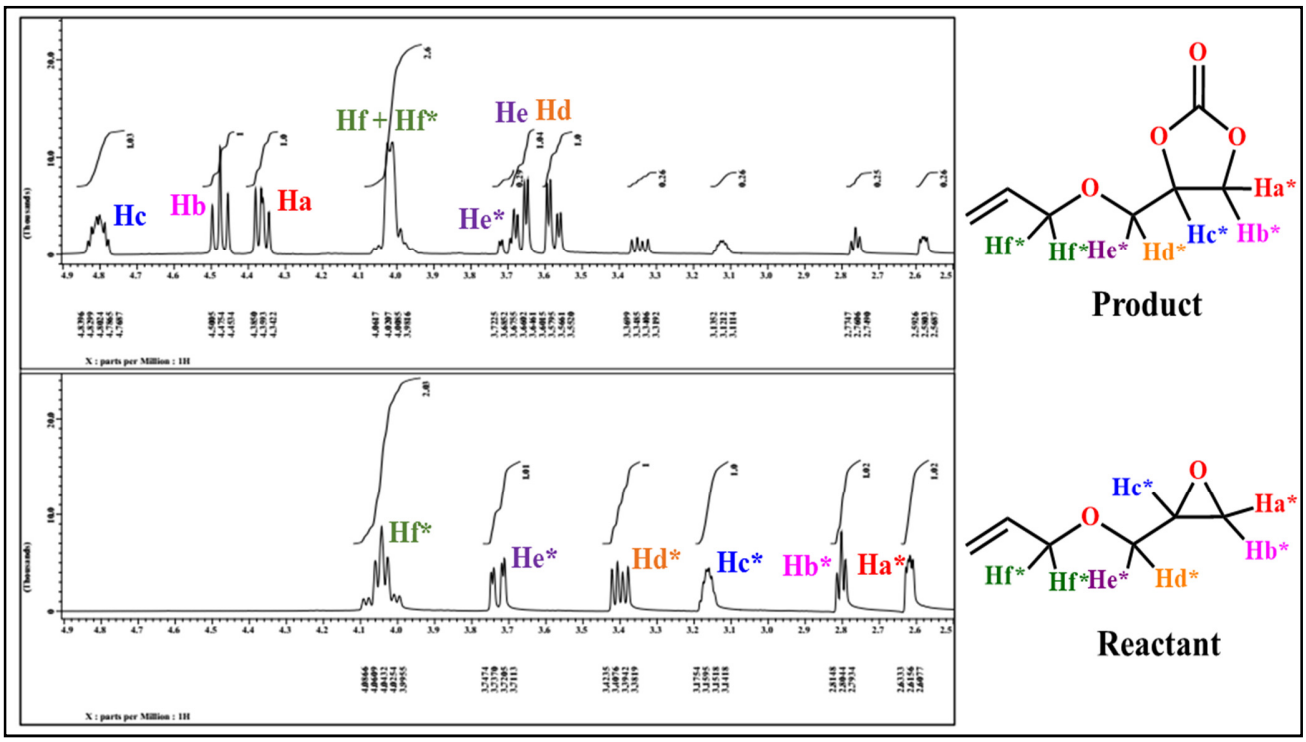

Figure S27. ^{1}H NMR ($CDCl_3$, 400 MHz) spectra for the cycloaddition reaction of allyl glycidyl ether with CO_2 catalyzed by MOF**1** (Table 2, entry no. 7).

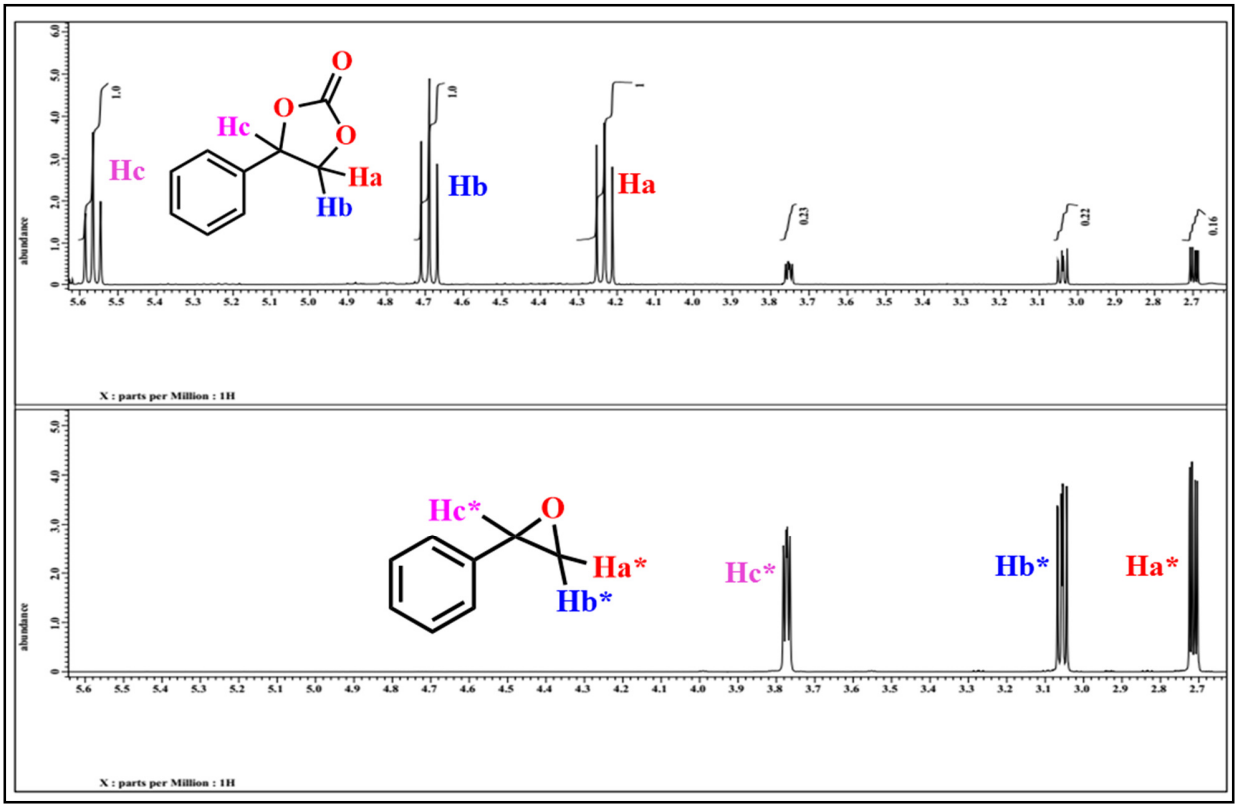

Figure S28. ^{1}H NMR ($CDCl_3$, 400 MHz) spectra for the cycloaddition reaction of styrene oxide with CO_2 catalyzed by MOF**1** (Table 2, entry no. 8).

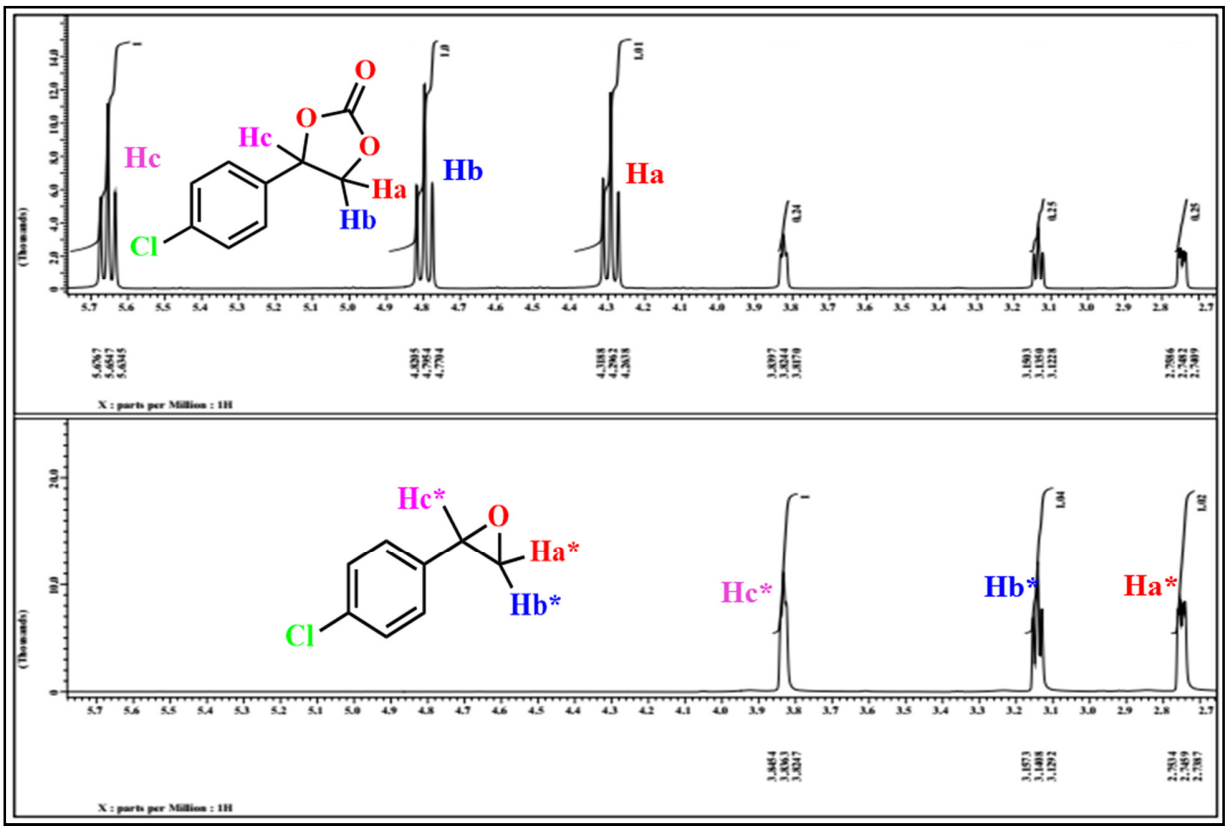

Figure S29. ^{1}H NMR ($CDCl_3$, 400 MHz) spectra for the cycloaddition reaction of *p*-chloro styrene oxide with CO_2 catalyzed by MOF**1** (Table 2, entry no. 9).

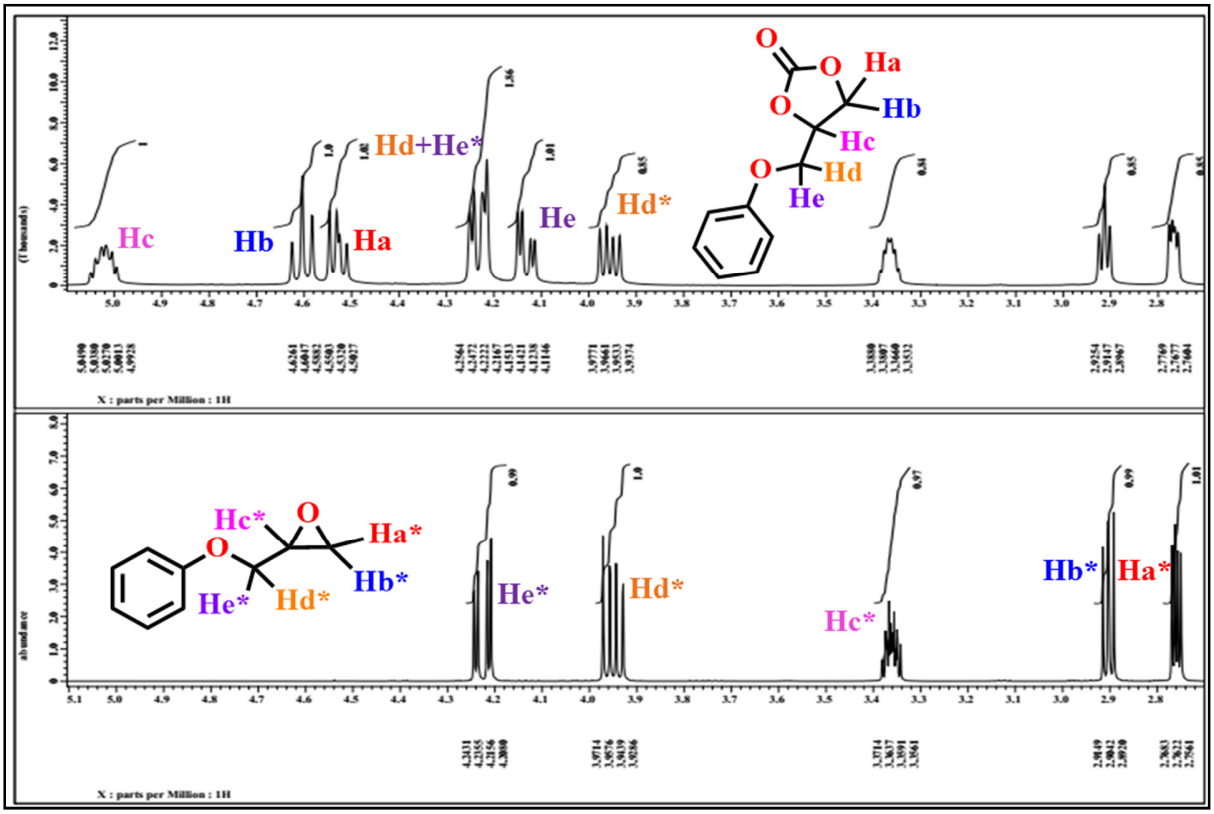

Figure S30. ^{1}H NMR ($CDCl_3$, 400 MHz) spectra for the cycloaddition reaction of phenyl glycidyl ether with CO_2 catalyzed by MOF**1** (Table 2, entry no. 10).

Table S5. Comparison of the reaction conditions used for cocatalyst-free CO_2 conversion by various MOFs reported in literature.

Sr. No.	MOF/Catalyst	Active site	Substrate	Reaction conditions	Con. (%)	Ref.
1.	Meim-UiO-66	$ZrOH/OH_2$, I^-	ECH,	1 bar, 120 °C, 24h	93	9
2.	UiO-67-IL	$ZrOH/OH_2$, I^-	ECH	1 bar, 90 °C, 8h	95	10
3.	IL-ZIF-90	Zn^{2+} and I^-	PO	10 bar, 120 °C, 3h	95	11
4.	F-IRMOF-3	Zn^{2+} and I^-	PO	20 bar, 140 °C, 15h	98	12
5.	F-ZIF-90	Zn^{2+} and I^-	ECH	11.7 bar, 120 °C, 6h	94	13
6.	MIL-101-N-(n-Bu)$_3$Br	Cr^{3+} and Br^-	PO	20 bar, 80 °C, 8 h	99	14
7.	MIL-101-P-(n-Bu)$_3$Br	Cr^{3+} and Br^-	PO	20 bar, 80 °C, 8 h	98	14
8.	Zn-TATAB	Zn^{2+} paddlewheel and NH	ECH	1 atm, 100 °C, 16h	95	15
9.	PolyILs@MIL-101	Cr^{3+} and Br^-	PO	1 bar, 45 °C, 48h	94	16
10.	IL@MIL-101-SO_3Na	Cr^{3+} and Br^-	ECH	1 atm, 90 °C, 36h	88	17
11.	IL/MIL-101-NH_2	Cr^{3+} and Cl^-	PO	13 bar, 120 °C, 1h	91	18
12.	Co-MOF1	Co^{2+} paddlewheel and NH	ECH	1 atm, 80 °C, 15h	93	**This work**

Substrate: PO = propylene oxide; ECH = epichlorohydrin.

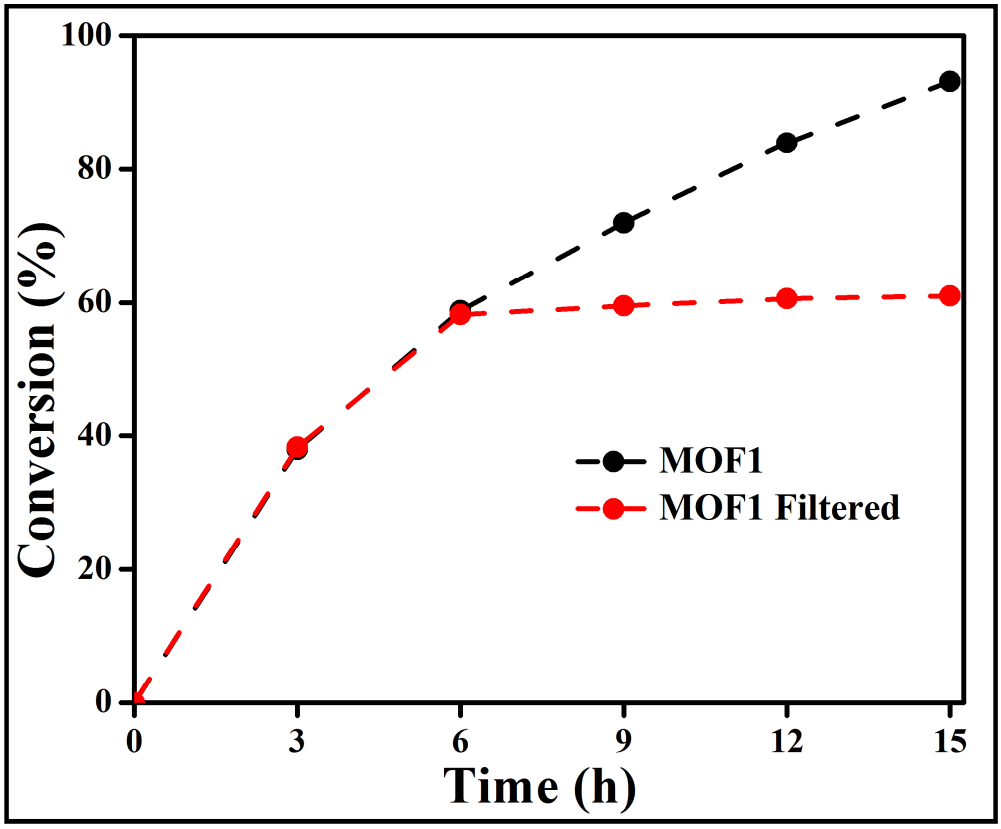

Figure S31. Leaching test for **MOF1**.

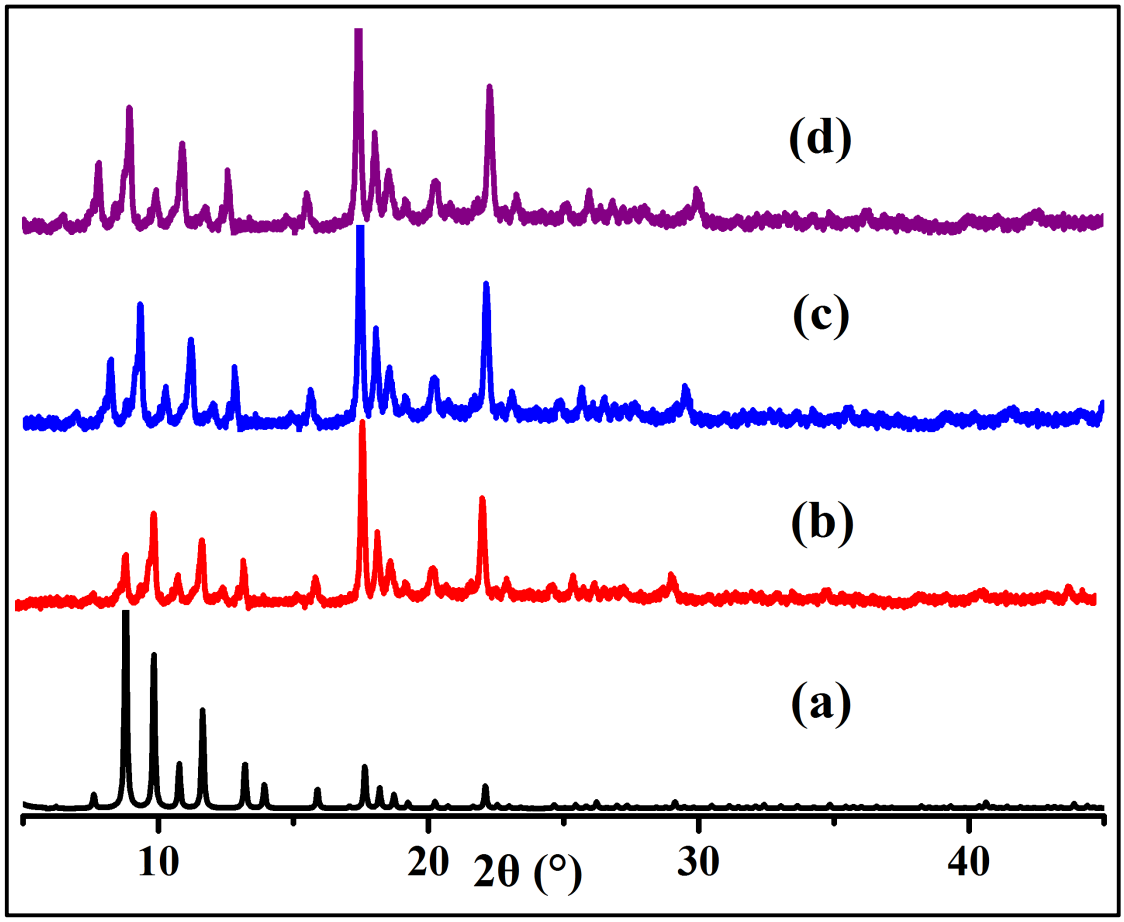

Figure S32. PXRD patterns of MOF**1** (a) pattern calculated from single crystal X- ray data; (b) as-synthesized sample before heating; (c) activated sample by heating at 150 °C for 20 hours; (d) sample recovered after five catalytic cycles.

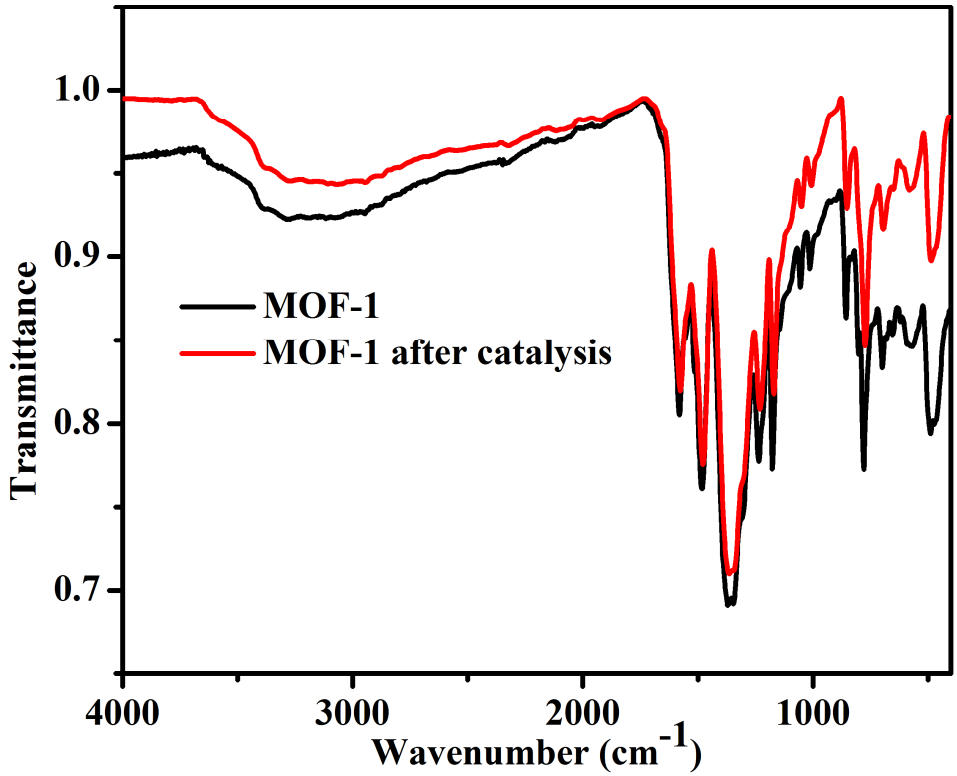

Figure S33. FT-IR spectra for as-synthesized and recovered sample of MOF**1** after catalysis.

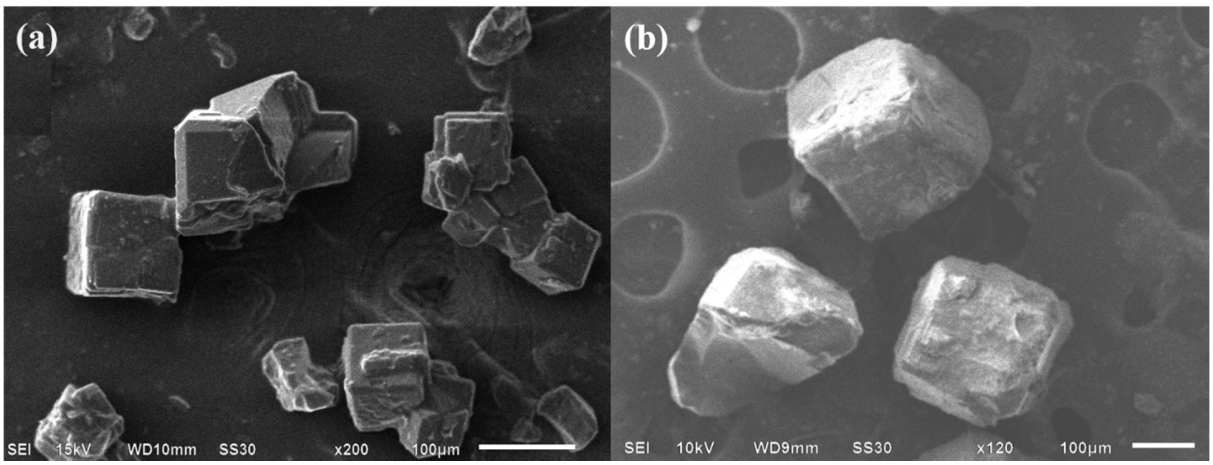

Figure S34. SEM images of MOF**1** (a) as-synthesised and (b) the sample recovered after catalysis showing retaining of the original morphology even after catalysis.

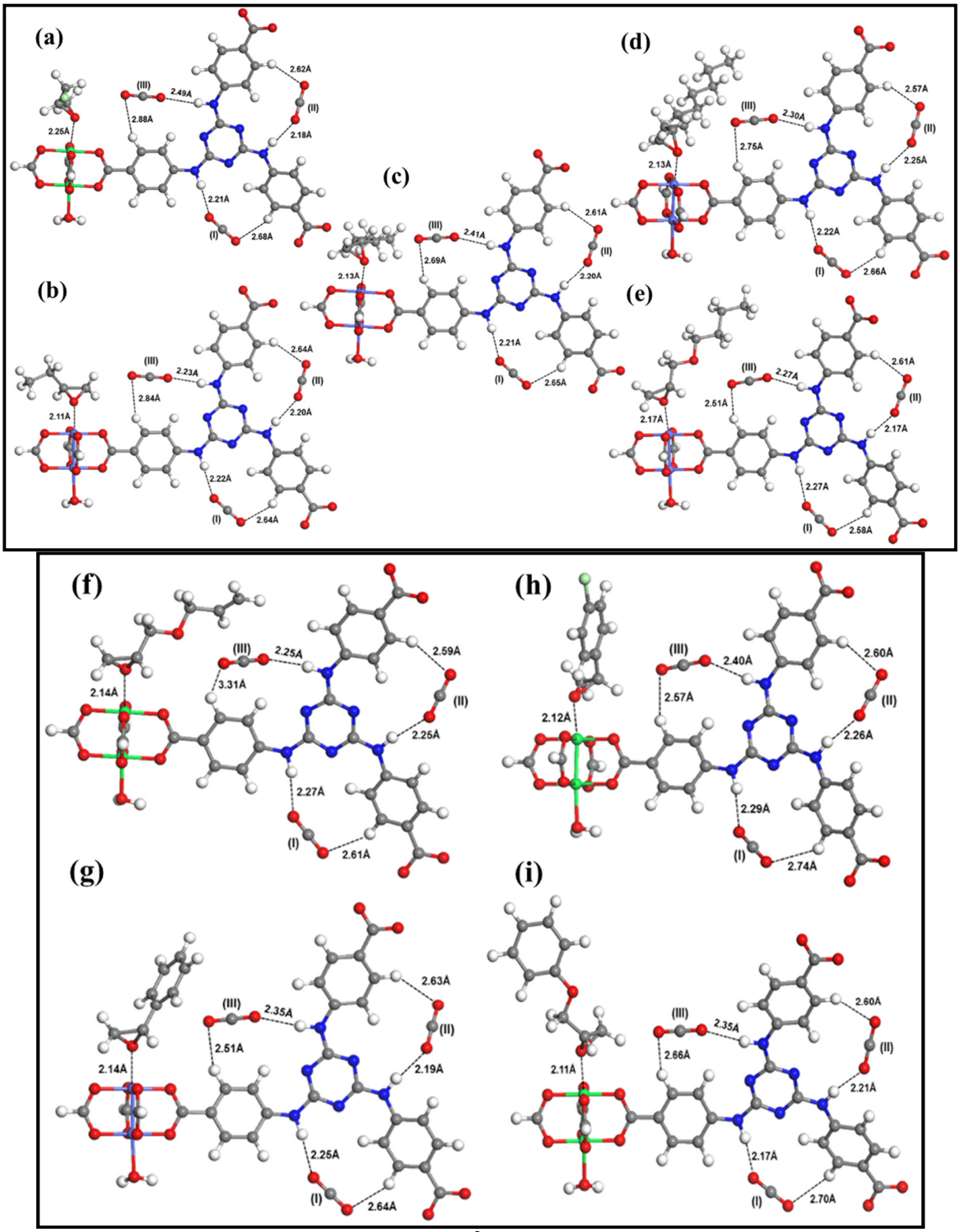

Figure S35. Optimized structures of $TATAB^{3-}$ ligand with a $\{Co_2(OOC)_4(H_2O)\}$ SBU with various epoxides showing the coordination of epoxides with Lewis acidic Co(II) center. Atom colors: Co-green; C-dark grey; O-Red; H-white and N-blue.

Table S6. Co-ordinates for the optimized structures of $TATAB^{3-}$ ligand and with three CO_2

$TATAB^{3-}$ ligand				**$TATAB^{3-}$ ligand with three CO_2**			
Co	17.98000000	0.07000000	13.90400000	Co	17.90900000	-0.03200000	13.93200000
Co	20.10500000	-0.51400000	14.38800000	Co	20.05700000	-0.56000000	14.38700000
O	20.19000000	0.86700000	15.72600000	O	20.10300000	0.76700000	15.77900000
O	18.04800000	1.45200000	15.24000000	O	17.93200000	1.27900000	15.33700000
O	22.16700000	-1.08000000	14.73100000	O	22.13200000	-1.11800000	14.68200000
H	22.23800000	-1.97700000	14.35600000	H	22.23200000	-1.94200000	14.16700000
C	19.14200000	1.56900000	15.88000000	C	19.02600000	1.41600000	15.97100000
O	17.89500000	-1.29800000	12.56500000	O	17.87400000	-1.33100000	12.51800000
O	18.62500000	1.32200000	12.57800000	O	18.50200000	1.31500000	12.67600000
O	17.33300000	-1.18500000	15.20600000	O	17.31000000	-1.36800000	15.17200000
O	20.02700000	-1.87800000	13.05000000	O	20.01800000	-1.86800000	12.99800000
O	20.76000000	0.72700000	13.06200000	O	20.66000000	0.76700000	13.11600000
O	19.47400000	-1.77400000	15.69300000	O	19.47300000	-1.88000000	15.65100000
H	22.67800000	-0.51200000	14.12600000	H	22.64000000	-0.45000000	14.18600000
C	18.93600000	-2.03000000	12.38400000	C	18.94100000	-2.01900000	12.31100000
C	18.88700000	-3.09800000	11.37300000	C	18.94500000	-3.03000000	11.24200000
C	17.72900000	-3.32500000	10.60500000	C	17.79400000	-3.29900000	10.48100000
C	20.00800000	-3.91600000	11.15500000	C	20.11400000	-3.76300000	10.97800000
C	17.69500000	-4.34600000	9.66500000	C	17.81300000	-4.28500000	9.50300000
C	19.98700000	-4.93900000	10.21700000	C	20.14700000	-4.75400000	10.00600000
C	18.82100000	-5.17500000	9.46000000	C	18.98400000	-5.04000000	9.26300000
N	18.71700000	-6.17200000	8.49100000	N	18.91300000	-6.02300000	8.27900000
H	17.88500000	-6.15400000	7.90400000	H	18.05700000	-6.04800000	7.72500000
C	19.54900000	-7.23300000	8.19300000	C	19.75400000	-7.07800000	7.99400000
N	20.63000000	-7.45500000	8.93800000	N	20.87500000	-7.25000000	8.69500000
N	19.14300000	-7.96400000	7.12900000	N	19.30500000	-7.86600000	6.99000000
C	21.36300000	-8.53100000	8.54600000	C	21.58400000	-8.35500000	8.34100000
C	19.96000000	-8.98600000	6.83700000	C	20.09800000	-8.91600000	6.73500000
N	21.09100000	-9.32700000	7.51100000	N	21.25700000	-9.22000000	7.37700000
N	22.45400000	-8.74000000	9.34700000	N	22.71400000	-8.52300000	9.09800000
N	19.69500000	-9.81200000	5.77700000	N	19.75900000	-9.81700000	5.76300000
H	22.49600000	-8.05700000	10.10000000	H	22.78900000	-7.81000000	9.82200000
C	23.52700000	-9.63800000	9.29200000	C	23.69400000	-9.52400000	9.13700000
H	20.39700000	-10.54500000	5.68900000	H	20.40500000	-10.60400000	5.72000000
C	18.66700000	-9.84300000	4.82500000	C	18.68300000	-9.86900000	4.86500000
C	23.68300000	-10.63200000	8.31000000	C	23.82900000	-10.54100000	8.17500000
C	24.50300000	-9.49400000	10.30100000	C	24.59700000	-9.46900000	10.22200000
C	17.61100000	-8.91200000	4.76500000	C	17.85300000	-8.77300000	4.55600000
C	18.72600000	-10.89000000	3.88000000	C	18.47900000	-11.10400000	4.21300000
C	24.80900000	-11.45100000	8.34300000	C	24.84200000	-11.48700000	8.31800000
C	25.61800000	-10.31800000	10.32100000	C	25.59800000	-10.42000000	10.35200000
C	16.63900000	-9.04700000	3.77700000	C	16.84600000	-8.92700000	3.60600000
C	17.75000000	-11.01200000	2.90200000	C	17.47200000	-11.24200000	3.27000000
C	25.78300000	-11.30500000	9.33900000	C	25.73000000	-11.44200000	9.40100000
C	16.69300000	-10.08900000	2.84200000	C	16.64500000	-10.15200000	2.95600000
C	26.99200000	-12.17300000	9.35500000	C	26.79900000	-12.46700000	9.54800000
C	15.64100000	-10.22800000	1.79800000	C	15.57000000	-10.29600000	1.93600000
O	27.21000000	-13.02600000	8.43900000	O	26.95700000	-13.39200000	8.69100000
O	27.85400000	-12.09300000	10.28400000	O	27.59400000	-12.45900000	10.53800000
O	14.71900000	-9.36500000	1.66200000	O	14.64700000	-9.43100000	1.82400000
O	15.62300000	-11.21700000	1.00200000	O	15.54700000	-11.28600000	1.14300000
O	15.97600000	0.63700000	13.31300000	O	15.87500000	0.47100000	13.39000000

H	16.09600000	1.44800000	12.78600000
H	15.72600000	-0.04800000	12.66500000
C	18.21200000	-1.86100000	15.82900000
C	19.88500000	1.39300000	12.42300000
H	17.84200000	-2.59400000	16.56400000
H	19.18200000	2.35800000	16.65000000
H	20.25500000	2.10200000	11.66500000
H	20.91100000	-3.74100000	11.73700000
H	20.85500000	-5.56900000	10.06000000
H	16.78800000	-4.51900000	9.08400000
H	16.85200000	-2.69900000	10.76200000
H	24.37800000	-8.72300000	11.06500000
H	26.37800000	-10.21200000	11.09700000
H	24.94500000	-12.22400000	7.58500000
H	22.92600000	-10.74000000	7.53900000
H	19.54400000	-11.61200000	3.92700000
H	17.78700000	-11.82100000	2.17200000
H	15.81500000	-8.33400000	3.72100000
H	17.56900000	-8.11000000	5.49400000

H	15.95500000	1.29500000	12.87400000
H	15.64400000	-0.21300000	12.73400000
C	18.21500000	-2.02300000	15.78000000
C	19.75900000	1.43300000	12.51600000
H	17.87500000	-2.78900000	16.49600000
H	19.04100000	2.17500000	16.77000000
H	20.09900000	2.18800000	11.78700000
H	21.00900000	-3.54200000	11.55600000
H	21.04800000	-5.32700000	9.81600000
H	16.91400000	-4.49400000	8.92300000
H	16.88300000	-2.73500000	10.67000000
H	24.49500000	-8.67500000	10.96400000
H	26.29500000	-10.38600000	11.19100000
H	24.95600000	-12.28200000	7.58100000
H	23.13300000	-10.57400000	7.34200000
H	19.12200000	-11.95000000	4.45700000
H	17.31100000	-12.19200000	2.75900000
H	16.19800000	-8.08900000	3.34900000
H	18.02000000	-7.82400000	5.05700000
C	15.47600000	-6.09600000	5.82600000
O	14.78400000	-6.53500000	4.99100000
O	16.16800000	-5.64200000	6.66500000
C	23.20500000	-5.39100000	12.08800000
O	23.10500000	-4.36100000	12.64200000
O	23.30700000	-6.41900000	11.53100000
C	22.65400000	-12.79700000	5.33100000
O	23.69900000	-13.24700000	5.60600000

Table S7. Co-ordinates for the optimized structures with different epoxides.

TATAB^{3-} ligand with Epichlorohydrin			
Co	17.99000000	0.08700000	13.75900000
Co	20.00200000	-0.69100000	14.44100000
O	20.08400000	0.66800000	15.81500000
O	18.07600000	1.46700000	15.10200000
C	19.09900000	1.47500000	15.85800000
O	17.89900000	-1.25700000	12.40200000
O	18.86300000	1.27600000	12.50400000
O	17.11600000	-1.08900000	14.99700000
O	19.91800000	-2.01200000	13.08600000
O	20.88400000	0.51700000	13.21200000
O	19.13700000	-1.88200000	15.66900000
C	18.89400000	-2.06800000	12.31400000
C	18.88000000	-3.12300000	11.29000000
C	17.75800000	-3.33700000	10.47000000
C	20.00700000	-3.94700000	11.12900000
C	17.76700000	-4.35000000	9.52300000
C	20.03000000	-4.96300000	10.18400000
C	18.90000000	-5.18200000	9.36800000
N	18.82600000	-6.17500000	8.39200000
H	17.98200000	-6.18700000	7.81800000
C	19.68200000	-7.21100000	8.08700000

TATAB^{3-} ligand with 1,2-epoxypropane			
Co	18.06600000	0.11300000	13.78200000
Co	19.88000000	-0.86300000	14.72500000
O	19.86500000	0.47500000	16.11900000
O	18.08700000	1.48800000	15.12600000
C	18.97600000	1.38000000	16.03000000
O	18.03000000	-1.23800000	12.43300000
O	19.22700000	1.19700000	12.67400000
O	16.90700000	-0.95000000	14.87500000
O	19.89600000	-2.16400000	13.32500000
O	21.04300000	0.26000000	13.66600000
O	18.72300000	-1.98200000	15.77400000
C	18.96100000	-2.12800000	12.44300000
C	18.95600000	-3.15400000	11.38800000
C	17.86500000	-3.28600000	10.50900000
C	20.04400000	-4.03200000	11.24700000
C	17.86400000	-4.26700000	9.52800000
C	20.06300000	-5.01100000	10.26200000
C	18.96200000	-5.14800000	9.38800000
N	18.87600000	-6.10700000	8.38000000
H	18.03500000	-6.08500000	7.80400000
C	19.70200000	-7.16700000	8.06900000

N 20.80300000 -7.38400000 8.78900000	N 20.81600000 -7.36700000 8.77100000
N 19.25500000 -7.98000000 7.06000000	N 19.25500000 -7.92500000 7.04000000
C 21.53300000 -8.46600000 8.40800000	C 21.52100000 -8.46600000 8.39400000
C 20.06800000 -9.00700000 6.77900000	C 20.04300000 -8.97400000 6.76500000
N 21.22500000 -9.31200000 7.42200000	N 21.19300000 -9.30700000 7.41100000
N 22.66700000 -8.62900000 9.16100000	N 22.64900000 -8.64600000 9.14800000
N 19.75300000 -9.87800000 5.77100000	N 19.71500000 -9.84900000 5.76500000
H 22.73700000 -7.92000000 9.88900000	H 22.73900000 -7.92200000 9.85800000
C 23.68100000 -9.59300000 9.15200000	C 23.66600000 -9.60600000 9.14100000
H 20.39000000 -10.67200000 5.72900000	H 20.35200000 -10.64300000 5.72600000
C 18.70300000 -9.88500000 4.84400000	C 18.66100000 -9.87300000 4.84300000
C 23.80200000 -10.60700000 8.18300000	C 23.75000000 -10.66900000 8.22200000
C 24.63300000 -9.50700000 10.19200000	C 24.65400000 -9.46500000 10.13900000
C 17.90300000 -8.76300000 4.55200000	C 17.81700000 -8.77700000 4.57300000
C 18.49300000 -11.09100000 4.14100000	C 18.49200000 -11.07700000 4.12300000
C 24.85200000 -11.51700000 8.27200000	C 24.81300000 -11.56600000 8.31400000
C 25.67400000 -10.42100000 10.26800000	C 25.70500000 -10.36500000 10.21800000
C 16.90900000 -8.86500000 3.58300000	C 16.82600000 -8.90300000 3.60300000
C 17.49500000 -11.18000000 3.18000000	C 17.49800000 -11.18700000 3.16100000
C 25.79300000 -11.43800000 9.30900000	C 25.79500000 -11.42500000 9.30300000
C 16.69100000 -10.06700000 2.89400000	C 16.65300000 -10.10000000 2.89300000
C 26.90200000 -12.42500000 9.40100000	C 26.92300000 -12.39200000 9.39800000
C 15.61100000 -10.16000000 1.87400000	C 15.58300000 -10.22100000 1.86400000
O 26.92400000 -13.46100000 8.66600000	O 26.93300000 -13.46500000 8.72000000
O 27.85900000 -12.26600000 10.22100000	O 27.91200000 -12.17400000 10.16400000
O 14.75200000 -9.23300000 1.73900000	O 14.67500000 -9.34000000 1.74800000
O 15.51400000 -11.16500000 1.10600000	O 15.54700000 -11.20900000 1.06700000
C 17.86700000 -1.84300000 15.69300000	C 17.47300000 -1.79400000 15.64000000
C 20.13400000 1.24600000 12.48800000	C 20.47800000 1.05400000 12.84800000
H 17.36600000 -2.53500000 16.39300000 H	H 16.81200000 -2.42800000 16.25200000
19.13800000 2.26200000 16.63000000	H 18.97500000 2.15300000 16.81600000
H 20.64000000 1.92000000 11.77400000	H 21.14000000 1.68100000 12.22700000
H 20.87600000 -3.77000000 11.76200000	H 20.88700000 -3.92600000 11.92900000
H 20.89700000 -5.60200000 10.06500000	H 20.90300000 -5.68700000 10.15300000
H 16.89000000 -4.52100000 8.89700000	H 17.00400000 -4.37600000 8.86500000
H 16.87800000 -2.70900000 10.59600000	H 17.00900000 -2.62000000 10.61500000
H 24.53600000 -8.71800000 10.94100000	H 24.57500000 -8.64500000 10.85600000
H 26.41000000 -10.36500000 11.07100000	H 26.47300000 -10.26500000 10.98600000
H 24.95900000 -12.30700000 7.52700000	H 24.90100000 -12.39000000 7.60600000
H 23.06500000 -10.65700000 7.38800000	H 22.98000000 -10.76600000 7.46100000
H 19.11900000 -11.95600000 4.36800000	H 19.14800000 -11.92200000 4.33600000
H 17.32400000 -12.11000000 2.63700000	H 17.35800000 -12.11500000 2.60700000
H 16.28300000 -8.00600000 3.34200000	H 16.16700000 -8.06500000 3.37500000
H 18.07900000 -7.83500000 5.08800000	H 17.96400000 -7.85000000 5.12000000
C 15.38100000 -6.26600000 5.85500000	C 15.39100000 -6.24500000 5.87900000
O 14.68400000 -6.62200000 4.98500000	O 14.69400000 -6.59800000 5.00900000
O 16.07800000 -5.89700000 6.73000000	O 16.08800000 -5.87800000 6.75500000
C 23.22500000 -5.27700000 12.36900000	C 23.28200000 -5.52300000 12.19600000
O 23.34500000 -4.37700000 13.11000000	O 23.44800000 -4.63200000 12.94000000
O 23.10600000 -6.17800000 11.62300000	O 23.11400000 -6.41400000 11.45100000
C 22.69800000 -12.84400000 5.41500000	C 22.68900000 -12.83100000 5.41700000
O 23.80800000 -13.21100000 5.35400000	O 23.79600000 -13.20400000 5.35000000
O 21.58000000 -12.48000000 5.47300000	O 21.57300000 -12.45900000 5.48300000
C 23.19700000 -0.82000000 14.91900000	O 16.37000000 1.02100000 12.76800000
H 24.01800000 -1.33500000 14.41400000	H 16.64800000 1.92400000 12.52800000
H 23.03000000 0.22700000 14.65500000	H 16.34500000 0.53000000 11.92600000

C	22.70900000	-1.32400000	16.21700000
C	23.35900000	-2.51900000	16.84100000
H	22.18200000	-0.63200000	16.87900000
H	23.68800000	-3.21800000	16.06200000
H	24.21500000	-2.22000000	17.46000000
O	21.98000000	-1.61500000	14.98800000
Cl	22.21300000	-3.40600000	17.91400000
O	16.08200000	0.81800000	13.05300000
H	16.14600000	1.78900000	13.04600000
H	16.06900000	0.55600000	12.11400000

$TATAB^{3-}$ ligand with 1, 2-epoxyhexane

Co	18.25400000	0.18600000	13.70400000
Co	20.03300000	-0.86900000	14.63300000
O	20.12900000	0.49100000	16.00200000
O	18.33500000	1.53700000	15.07800000
C	19.25400000	1.41400000	15.94700000
O	18.16000000	-1.13800000	12.32200000
O	19.43900000	1.24400000	12.60200000
O	17.05300000	-0.85200000	14.77900000
O	19.92800000	-2.18700000	13.27000000
O	21.21800000	0.18500000	13.53100000
O	18.83200000	-1.89000000	15.74000000
C	19.02800000	-2.08800000	12.36100000
C	19.00700000	-3.12200000	11.31300000
C	17.98400000	-3.17000000	10.34900000
C	20.02800000	-4.08600000	11.26700000
C	17.98300000	-4.16200000	9.37700000
C	20.04400000	-5.07700000	10.29300000
C	19.00800000	-5.13500000	9.33700000
N	18.91600000	-6.10700000	8.34000000
H	18.09400000	-6.06000000	7.73800000
C	19.71200000	-7.19500000	8.06200000
N	20.81600000	-7.41500000	8.77800000
N	19.26000000	-7.95700000	7.03700000
C	21.50800000	-8.52300000	8.40800000
C	20.02700000	-9.02400000	6.78200000
N	21.17000000	-9.36700000	7.43200000
N	22.64000000	-8.71700000	9.15700000
N	19.68700000	-9.91300000	5.79600000
H	22.73800000	-8.01000000	9.88400000
C	23.66800000	-9.66100000	9.09300000
H	20.31400000	-10.71800000	5.77500000
C	18.64500000	-9.94000000	4.86600000
C	23.79700000	-10.62900000	8.07700000
C	24.64100000	-9.58700000	10.11600000
C	17.79300000	-8.84900000	4.58700000
C	18.49000000	-11.15000000	4.14800000
C	24.88800000	-11.49400000	8.09500000
C	25.72400000	-10.45300000	10.11800000
C	16.80900000	-8.98800000	3.61300000
C	17.50500000	-11.27100000	3.18200000
C	25.85900000	-11.42100000	9.10700000
C	16.64900000	-10.19100000	2.90300000
C	22.64700000	-2.30900000	14.94600000
C	22.80600000	-1.13700000	15.81800000
H	22.56900000	-2.17300000	13.86500000
H	22.98500000	-3.28900000	15.29100000
H	22.82000000	-0.16100000	15.32200000
O	21.50000000	-1.80200000	15.68900000
C	23.38300000	-1.19700000	17.20400000
H	24.47600000	-1.07100000	17.13700000
C	22.76500000	-0.11200000	18.09000000
H	21.66900000	-0.20000000	18.08300000
H	23.12200000	-0.18700000	19.12600000
H	23.02500000	0.88800000	17.71100000
H	23.19600000	-2.19800000	17.62200000

$TATAB^{3-}$ ligand with 1, 2-epoxydecane

Co	18.17700000	0.30400000	13.75300000
Co	20.03000000	-0.64000000	14.65700000
O	20.12400000	0.79000000	15.95400000
O	18.21400000	1.67700000	15.10100000
C	19.18400000	1.64900000	15.91800000
O	18.12600000	-1.04800000	12.40000000
O	19.28800000	1.39900000	12.61300000
O	17.04900000	-0.77800000	14.86300000
O	19.93900000	-2.02200000	13.35000000
O	21.14000000	0.39400000	13.45900000
O	18.89900000	-1.64600000	15.85400000
C	19.02900000	-1.96700000	12.44700000
C	19.02900000	-3.01500000	11.41400000
C	17.93300000	-3.18800000	10.54900000
C	20.14000000	-3.86700000	11.28200000
C	17.94400000	-4.20000000	9.60100000
C	20.17100000	-4.87300000	10.32300000
C	19.05700000	-5.06400000	9.47500000
N	18.97000000	-6.05100000	8.49500000
H	18.12300000	-6.04100000	7.92800000
C	19.78900000	-7.11500000	8.18600000
N	20.91000000	-7.32300000	8.87900000
N	19.32000000	-7.86800000	7.16200000
C	21.60100000	-8.42500000	8.48200000
C	20.10100000	-8.91500000	6.86700000
N	21.25700000	-9.25200000	7.49400000
N	22.74000000	-8.64200000	9.21400000
N	19.76800000	-9.78200000	5.86200000
H	22.86100000	-7.94300000	9.94500000
C	23.71700000	-9.64300000	9.17000000
H	20.42500000	-10.55900000	5.80100000
C	18.71300000	-9.81700000	4.94200000
C	23.77700000	-10.66200000	8.19700000
C	24.69900000	-9.59300000	10.18300000
C	17.77300000	-8.78400000	4.75900000
C	18.64000000	-10.97500000	4.14000000
C	24.80500000	-11.60100000	8.25400000
C	25.71800000	-10.53400000	10.22600000
C	16.78700000	-8.92600000	3.78600000
C	17.65300000	-11.10100000	3.17500000
C	25.78200000	-11.54900000	9.25800000

C 27.02700000 -12.35400000 9.10700000	C 16.71500000 -10.07500000 2.98800000
C 15.58300000 -10.33200000 1.86600000	C 26.88300000 -12.55000000 9.30000000
O 26.88700000 -13.52100000 8.63800000	C 15.65900000 -10.20800000 1.94600000
O 28.13300000 -11.95700000 9.57900000	O 26.81800000 -13.62900000 8.63400000
O 14.49300000 -9.70500000 2.01000000	O 27.92000000 -12.35100000 10.00400000
O 15.79000000 -11.08000000 0.86600000	O 14.72800000 -9.35100000 1.83200000
C 17.58800000 -1.68100000 15.58100000	O 15.65800000 -11.18000000 1.12900000
C 20.68400000 1.02500000 12.74300000	C 17.64300000 -1.52900000 15.69900000
H 16.89900000 -2.27900000 16.20200000	C 20.54300000 1.20700000 12.68800000
H 19.30300000 2.18600000 16.73300000	H 17.00300000 -2.14200000 16.35500000
H 21.36900000 1.62400000 12.11900000	H 19.21600000 2.44900000 16.67700000
H 20.81500000 -4.04400000 12.01800000	H 21.17900000 1.81200000 12.02100000
H 20.83400000 -5.81800000 10.25700000	H 20.99000000 -3.71700000 11.94700000
H 17.18600000 -4.20000000 8.63300000	H 21.02800000 -5.52900000 10.21600000
H 17.18800000 -2.42700000 10.37500000	H 17.08100000 -4.34300000 8.94900000
H 24.53500000 -8.83200000 10.89900000	H 17.06800000 -2.53200000 10.64100000
H 26.48700000 -10.39300000 10.89400000	H 24.64800000 -8.80700000 10.93900000
H 24.99900000 -12.25600000 7.32300000	H 26.48000000 -10.50100000 11.00400000
H 23.04300000 -10.67400000 7.29700000	H 24.87000000 -12.39000000 7.50500000
H 19.15200000 -11.98800000 4.37000000	H 23.01800000 -10.69100000 7.42200000
H 17.38200000 -12.19700000 2.62100000	H 19.37000000 -11.77300000 4.28700000
H 16.13500000 -8.16100000 3.38900000	H 17.59100000 -11.99600000 2.55400000
H 17.92500000 -7.92100000 5.13700000	H 16.05100000 -8.13600000 3.62700000
C 15.42700000 -6.25100000 5.89900000	H 17.84400000 -7.89100000 5.37300000
O 14.73100000 -6.62800000 5.03800000	C 15.44100000 -6.12200000 6.11000000
O 16.12500000 -5.86200000 6.76500000	O 14.74400000 -6.47400000 5.23800000
C 23.22000000 -5.52600000 12.37700000	O 16.13600000 -5.75900000 6.98700000
O 23.23200000 -4.57300000 13.06000000	C 23.46200000 -5.45000000 12.21700000
O 23.20600000 -6.48100000 11.69200000	O 23.46400000 -4.47400000 12.86600000
C 2.62100000 -12.92300000 5.38300000	O 23.46000000 -6.42800000 11.56600000
O 23.72300000 -13.31000000 5.30800000	C 22.72300000 -12.83200000 5.39700000
O 21.51100000 -12.53700000 5.45500000	O 23.82000000 -13.23300000 5.32000000
O 16.63700000 1.23800000 12.72900000	O 21.62000000 -12.43100000 5.47300000
H 17.03300000 2.10600000 12.52800000	O 16.45200000 1.20500000 12.80400000
H 16.58100000 0.78300000 11.86800000	H 16.81400000 1.94700000 12.28500000
C 22.09900000 -1.73400000 16.84700000	H 16.18900000 0.53800000 12.14300000
C 23.01300000 -1.93600000 15.71200000	C 22.19200000 -1.32500000 16.84700000
H 21.95100000 -2.52800000 17.58600000	C 23.05900000 -1.64300000 15.70100000
H 21.87200000 -0.71400000 17.17200000	H 22.04600000 -2.05200000 17.65100000
H 23.48600000 -2.92100000 15.61800000	H 22.00900000 -0.27600000 17.09600000
O 21.55900000 -2.05800000 15.53300000	H 23.50300000 -2.64500000 15.67600000
C 23.74800000 -0.81600000 15.03400000	O 21.60000000 -1.74000000 15.58200000
H 24.66900000 -0.64400000 15.61900000	C 23.80300000 -0.60700000 14.90800000
C 24.12600000 -1.14000000 13.58700000	H 24.74500000 -0.41500000 15.45400000
H 23.15100000 0.10900000 15.08500000	C 24.13400000 -1.09600000 13.49400000
H 23.20900000 -1.23900000 12.98600000	H 23.23500000 0.33500000 14.89200000
C 25.03700000 -0.08100000 12.96600000	H 23.22500000 -1.06800000 12.87000000
C 25.44900000 -0.43200000 11.53500000	C 25.27300000 -0.32200000 12.82800000
H 26.15000000 0.30800000 11.12200000	C 25.77700000 -1.01200000 11.55800000
H 25.94500000 -1.41600000 11.50900000	H 25.93000000 -2.08400000 11.78100000
H 24.57400000 -0.48300000 10.86800000	H 25.00100000 -0.97000000 10.77400000
H 24.52900000 0.90000000 12.99200000	H 24.96500000 0.71500000 12.60400000
H 25.94300000 0.02300000 13.58800000	H 26.11200000 -0.24700000 13.54400000
H 24.63600000 -2.11900000 13.55400000	H 24.44200000 -2.15300000 13.54900000
	C 27.09100000 -0.44300000 11.02300000
	C 27.65100000 -1.24400000 9.84700000

	C 29.01800000 -0.74800000 9.37300000 C 29.59400000 -1.58200000 8.22800000 H 30.58500000 -1.21600000 7.92100000 H 29.70000000 -2.63700000 8.52900000 H 28.93400000 -1.55100000 7.34500000 H 28.93400000 0.30700000 9.05900000 H 29.71500000 -0.75900000 10.22900000 H 27.73500000 -2.30600000 10.14300000 H 26.93500000 -1.21600000 9.00700000

References

1. *SMART (V 5.628), SAINT (V 6.45a), XPREP, SHELXTL*; Bruker AXS Inc. Madison, Wisconsin, USA, **2004**.

2. Sheldrick, G. M. *Siemens Area Detector Absorption Correction Program,* University of Göttingen, Göttingen, Germany, **2004**.

3. Altomare, A.; Cascarano, G.; Giacovazzo, C.; Guagliardi, A. SIR92 – a program for automatic solution of crystal structures by direct methods. *J. Appl. Crystallogr*. **1993**, *26*, 343-350.

4. Sheldrick, G. M. *SHELXL-2014, Program for Crystal Structure Solution and Refinement;* University of Göttingen, Göttingen, Germany, **2014**.

5. Farrugia, L. J. WinGX-A *Windows Program for Crystal Structure Analysis. J. Appl. Crystallogr*. **2012**, *45*, 849-854.

6. Spek, A. L. Single-crystal structure validation with the program PLATON *J. Appl. Crystallogr.* **2003**, *36*, 7-13.

7. a) Pan, H. Ritter, J. A. Balbuena, P. B. Examination of the approximations used in determining the isosteric heat of Adsorption from the Clausius-Clapeyron equation. *Langmuir* **1998**, *14*, 6323 -6327. b) N. Sikdar, A. Hazra, T. K. Maji, Stoichiometry-controlled two flexible interpenetrated frameworks: Higher CO_2 uptake in a nanoscale counterpart supported by accelerated adsorption kinetics. *Inorg. Chem*. **2014**, *53*, 5993-6002.

8. Yang, R. T. *Gas Separation by Adsorption Processes*, Butterworth, Boston, **2003**.

9. Liang, J.; Chen, R. P.; Wang, X. Y.; Liu, T. T.; Wang, X. S.; Huang, Y. B.; Cao, R. Postsynthetic ionization of an imidazole-containing metal–organic framework for the cycloaddition of carbon dioxide and epoxides. *Chem. Sci.* **2017**, *8*, 1570-1575.

10. Ding, L. G.; Yao, B. J.; Jiang, W. L.; Li, J. T.;. Fu, Q. J; Li, Y. A.; Liu, Z .H.; Ma, J. P.; Dong, Y. B. Bifunctional imidazolium-based ionic liquid decorated UiO-67 type MOF for selective CO_2 adsorption and catalytic property for CO_2 cycloaddition with epoxides. *Inorg. Chem.* **2017**, *56*, 2337–2344.

11. Tharun, J.; Bhin, K.; Roshan, R.; Kim, D.; Kathalikkattil, A.; Babu, R.; Ahn, H.Y.; Won, Y. Park, D. W. Ionic liquid tethered post functionalized ZIF-90 framework for the cycloaddition of propylene oxide and CO_2. *Green Chem.* **2016**, *18*, 2479–2487.

12. Zhou, X.; Zhang, Y.; Yang, X.; Zhao, L.; Wang, G. Functionalized IRMOF-3 as efficient heterogeneous catalyst for the synthesis of cyclic carbonates. *J. Mol. Catal. A: Chem.* **2012**, *12*, 361–362.

13. Jose, T.; Hwang, Y.; Kim, D. W.; Kim, M. I.; Park, D. W. Functionalized zeolitic imidazolate framework F-ZIF-90 as efficient catalyst for the cycloaddition of carbon dioxide to allyl glycidyl ether. *Catal. Today* **2015**, *245*, 61-69.

14. Ma, D.; Li, B.; Liu, K.; Zhang, X.; Zou, W.; Yang, Y.; Li, G.; Shi, Z.; Feng, S. Bifunctional MOF heterogeneous catalysts based on the synergy of dual functional sites for efficient conversion of CO_2 under mild and co-catalyst free conditions. *J. Mater. Chem. A* **2015**, *3*, 23136-23142.

15. Han, Y. H.; Zhou, Z. Y.; Tian, C. B.; Du. S. W. A dual-walled cage MOF as an efficient heterogeneous catalyst for the conversion of CO_2 under mild and co-catalyst free conditions. *Green Chem*. **2016**, *18*, 4086-4091.

16. Ding, M.; Jiang, H. L. Incorporation of imidazolium-based poly(ionic liquid)s into a metal–organic framework for CO_2 capture and conversion. *ACS Catal.* **2018**, *8*, 3194–3201.

17. Y. Sun, H. Huang, H. Vardhan, B. Aguila, C. Zhong, J. A. Perman, A. M. Al-Enizi, A. Nafady, S. Ma, Facile approach to graft ionic liquid into MOF for improving the efficiency of CO_2 chemical fixation. *ACS Appl. Mater. Interfaces* **2018**, *10*, 27124–27130.

18. Wang, T.; Song, X.; Luo, Q.; Yang, X.; Chong, S.; Zhang, J.; Ji, M. Acid-base bifunctional catalyst: carboxyl ionic liquid immobilized on MIL-101-NH_2 for rapid synthesis of propylene carbonate from CO_2 and propylene oxide under facile solvent-free conditions. *Microporous and Mesoporous Mater.* **2018**, *267*, 84–92.